A Generalization of Wirtinger Flow for Exact Interferometric Inversion

Bariscan Yonel, Birsen Yazici

Electrical & Computer Systems Engineering, Rensselaer Polytechnic Institute, Troy, NY

Abstract

Interferometric inversion involves recovery of a signal from cross-correlations of its linear transformations. A close relative of interferometric inversion is the generalized phase retrieval problem, which consists of recovering a signal from the auto-correlations of its linear transformations. Recently, significant advancements have been made in phase retrieval methods despite the ill-posed, and non-convex nature of the problem. One such method is Wirtinger Flow (WF) [1], a non-convex optimization framework that provides high probability guarantees of exact recovery under certain measurement models, such as coded diffraction patterns, and Gaussian sampling vectors. In this paper, we develop a generalization of WF for interferometric inversion, which we refer to as Generalized Wirtinger Flow (GWF). GWF theory extends the probabilistic exact recovery results in [1] to arbitrary measurement models characterized in the equivalent lifted problem, hence covers a larger class of measurement models. GWF framework unifies the theory of low rank matrix recovery (LRMR) and the non-convex optimization approach of WF, thereby establishes theoretical advantages of the non-convex approach over LRMR. We show that the conditions for exact recovery via WF can be derived through a low rank matrix recovery formulation. We identify a new sufficient condition on the lifted forward model that directly implies exact recovery conditions of standard WF. This condition is less stringent than those of LRMR, which is the state of the art approach for exact interferometric inversion. We next establish our sufficient condition for the cross-correlations of linear measurements collected by complex Gaussian sampling vectors. In the particular case of the Gaussian model, we show that the exact recovery conditions of standard WF imply our sufficient condition, and that the regularity condition of WF is redundant for the interferometric inversion problem. Finally, we demonstrate the effectiveness of GWF numerically in a deterministic multi-static radar imaging scenario.

Key words— interferometric inversion, Wirtinger Flow, phase retrieval, wave-based imaging, interferometric imaging, low rank matrix recovery, PhaseLift

1 Introduction

Interferometric inversion involves the recovery of a signal of interest from the cross-correlations of its linear measurements, each collected by a different sensing process. Let $\mathbf{L}_i^m, \mathbf{L}_j^m \in \mathbb{C}^N$ denote the m^{th} sampling vectors of the i^{th} and j^{th} sensing processes and $\boldsymbol{\rho}_t \in \mathbb{C}^N$ be the signal of interest. We define

$$f_i^m = \langle \mathbf{L}_i^m, \boldsymbol{\rho}_t \rangle, \quad f_j^m = \langle \mathbf{L}_i^m, \boldsymbol{\rho}_t \rangle, \quad m = 1, \cdots, M,$$
 (1)

as the linear measurements and describe cross-correlated measurements as

$$d_{ij}^{m} = f_{i}^{m} \overline{f_{j}^{m}} = (\mathbf{L}_{i}^{m})^{H} \boldsymbol{\rho}_{t} \boldsymbol{\rho}_{t}^{H} \mathbf{L}_{j}^{m} \quad m = 1, \cdots M,$$
(2)

where $\overline{(\cdot)}$ denotes complex conjugation. Thus, interferometric inversion involves recovery of $\rho_t \in \mathbb{C}^N$ from $d_{ij}^m \in \mathbb{C}$, m = 1, ..., M using the model in (2).

Interferometric inversion problem arises in many applications in different disciplines. These include radar and sonar interferometry [2–4], passive imaging in acoustic, electromagnetic and geophysical applications [5–20], interferometric microscopy [21], beamforming and sensor localization in large area networks [22], [23–25] among others. Cross-correlation of measurements were shown to provide robustness to statistical fluctuations in scattering media or incoherent sources in wave-based imaging [26, 27], and with respect to phase errors in the correlated linear transformations [28–31]. Therefore, in applications such as passive imaging [5–20] and interferometry [2–4], cross-correlations are formed as a part of the inference process after acquiring linear measurements by sensors that are configured differently in space, time or frequency. Additionally, the cross-correlated measurement model arises naturally from the underlying physical sensing processes in certain applications such as optical and radio astronomy [32, 33], or quantum optical imaging [34].

A special case of the interferometric inversion problem is when i = j in (2), in which the measurement model becomes the auto-correlations of linear measurements collected by a single sensing process. In this case, the interferometric inversion problem reduces to the well-known phase retrieval problem. Notably, both problems are non-convex quadratic programs due to the equality constraints enforced by the correlated measurement model. In recent years, several phase retrieval methods with exact recovery guarantees have been developed despite the non-convex nature of the problem. These methods are characterized by either one or both of the following two principles: convexification of the solution set, which includes lifting based approaches [35–37], or a provably accurate initialization, followed by an algorithmic map that refines the initial estimate, which is most prominently established by Wirtinger Flow (WF) [1].

In methods that deploy lifting, such as PhaseLift [35, 36], signal recovery from quadratic measurements is reformulated as a low rank matrix recovery (LRMR) problem. While the LRMR approach offers convergence guarantees via convexification, it has limited practical applicability in typical sensing and imaging problems since lifting increases the dimension of the inverse problem by an order of magnitude and requires demanding memory storage in implementation. The WF framework, on the other hand, avoids lifting, hence offers advantages in computational complexity and memory requirements. Despite solving the non-convex quadratic program directly, convergence to a global solution at a geometric rate is guaranteed by WF for coded diffraction patterns and Gaussian sampling vectors [1], and more recently for short time Fourier transforms [38]. These advantages promote WF as a theoretical framework suitable for large scale imaging problems, and also inspired several of its variants [38–45].

Conventionally, interferometric inversion in imaging applications has been approached by Fourier based techniques, such as time or frequency difference of arrival (TDOA/FDOA) backprojection [5, 6, 9, 13, 16, 18, 19, 46]. While these methods are practical and computationally efficient, their applicability is limited due to underlying assumptions. As an alternative, LRMR has been explored for interferometric inversion [11, 47]. The LRMR approach is inspired by the PhaseLift method [35,36] and suffers from the drawbacks of increased computational complexity and memory

requirements.

In this paper, motivated by the advantages offered by WF, we develop a generalization of WF for the interferometric inversion problem with exact recovery guarantees, which we refer to as the Generalized Wirtinger Flow (GWF). Our framework differs from the standard WF in the following ways: i) GWF provides exact recovery guarantees to a larger class of problems than that of standard WF. This class is characterized by the forward map of the lifted problem satisfying restricted isometry property (RIP) on the set of rank-1, positive semi-definite (PSD) matrices (RIP-1). Furthermore, we provide an upper bound for the restricted isometry constant (RIC) so that RIP-1 is a sufficient condition for convergence to a global solution. ii) GWF theory is established in the lifted domain. This lifting-based perspective allows us to develop an alternative framework for exact recovery guarantees that bridges the theory between LRMR and the non-convex approach of WF. As a result, the arguments used for Gaussian and coded diffraction pattern (CDP) sampling vectors are extended to arbitrary measurement models that satisfy our sufficient condition in the equivalent lifted problem.

Our approach results in a deterministic framework. Hence, GWF offers exact recovery guarantees to deterministic interferometric inversion problems that are widely encountered in real-world applications. One such application is phaseless array imaging, for which it was shown that the RIP-1 condition is satisfied for sufficiently high central frequencies [48]. In addition, by developing GWF through the equivalent lifted problem, we identify the key theoretical advantages of the non-convex approach over LRMR beyond the immediate gains in computation and applicability. Our exact recovery condition for GWF proves to be a less stringent restricted isometry property than that of the sufficient conditions of PhaseLift, which have to hold over the full positive semi-definite cone, as opposed to only over its rank-1 elements. Accordingly, we consider GWF as an exact interferometric imaging method alternative to LRMR, and motivate multi-static radar imaging as a suitable application by [49].

In our key results, we establish that the GWF sufficient condition directly implies the exact recovery conditions of standard WF. Specifically, we show that the RIP-1 property on the lifted forward model implies an accurate initialization by the spectral method and ensures that the WF regularity condition for convergence is satisfied in the ϵ -neighborhood defined by the initialization. Next, despite that the RIP-1 condition in the lifted problem does not apply for the case of auto-correlations and the analysis in [1], we show this property is satisfied for cross-correlation of linear measurements collected by i.i.d. Gaussian sampling vectors. To validate our analysis we conduct numerical experiments for the Gaussian sampling model by counting empirical probability of exact recovery. We next demonstrate the effectiveness of GWF in a realistic passive multi-static radar imaging scenario. Despite the asymptotic status of our RIP-1 result for multi-static radar imaging, our numerical simulations strongly agree with our theoretical results and show that the interferometric inversion is solved in an exact manner by GWF.

The rest of our paper is organized as follows. We begin by formulating the GWF algorithm in Section 2, present key definitions and terminology followed by the main theorem statements in Section 3. The proofs of the main theorems are provided in Section 4. The numerical simulations for Gaussian sampling model and interferometric multi-static radar imaging are presented in Section 5. Section 6 concludes our paper. Appendices A, B, and C include proofs of lemmas used in Section 3.

2 Generalized Wirtinger Flow Algorithm

2.1 The Non-Convex Objective Function

To address the interferometric inversion problem, we define the following objective function, and set up the corresponding optimization problem:

$$\mathcal{J}(\boldsymbol{\rho}) := \frac{1}{2M} \sum_{m=1}^{M} |\left(\mathbf{L}_{i}^{m}\right)^{H} \boldsymbol{\rho} \boldsymbol{\rho}^{H} \mathbf{L}_{j}^{m} - d_{ij}^{m}|^{2}, \tag{3}$$

$$\hat{\boldsymbol{\rho}} = \underset{\boldsymbol{\rho}}{\operatorname{argmin}} \ \mathcal{J}(\boldsymbol{\rho}). \tag{4}$$

Let $\mathbf{y} = [y_{ij}^1, y_{ij}^2, \cdots y_{ij}^M]^T$ and $\mathcal{L} : \mathbb{C}^N \to \mathbb{C}^M$ be the cross-correlated measurement map defined as

$$\mathcal{L}(\boldsymbol{\rho}) = \mathbf{y}, \text{ where } \boldsymbol{\rho} \in \mathbb{C}^N, \ \ y_{ij}^m = (\mathbf{L}_i^m)^H \boldsymbol{\rho} \boldsymbol{\rho}^H \mathbf{L}_j^m.$$
 (5)

The objective function in (3) is the ℓ_2 mismatch in the range of \mathcal{L} , i.e., the space of cross-correlated measurements, and the minimization in (4) is equivalent to solving the perturbed problem of quadratic equality constraints of (2) over the signal domain \mathbb{C}^N . The main obstacle in solving (4) is that the objective function \mathcal{J} is non-convex over the variable ρ due to the invariance of cross-correlated measurements to global phase factors. Essentially (4) has a non-convex solution set with infinitely many elements, which casts interferometric inversion a challenging, ill-posed problem.

Definition 2.1 (Global Solution Set). We say that the points

$$P := \{ e^{i\Phi} \boldsymbol{\rho}_t : \Phi \in [0, 2\pi) \},$$

form the global solution set for the interferometric inversion from the cross-correlated measurements (2).

More generally, for any $\rho \in \mathbb{C}^N$, let $\mathcal{E}_{\rho} = \{\mathbf{z} \in \mathbb{C}^N : \mathcal{L}(\mathbf{z}) = \mathcal{L}(\rho)\}$ be the equivalence class of ρ under \mathcal{L} . We then define the following collection of signals as the *equivalence set* of ρ .

Definition 2.2 (Equivalence Set). Let $\rho \in \mathbb{C}^N$ and

$$P_{\boldsymbol{\rho}} := \{ e^{i\Phi} \boldsymbol{\rho}, \Phi \in [0, 2\pi) \}, \tag{6}$$

We refer to P_{ρ} as the equivalence set of ρ .

Remark. Note that $P_{\rho} \subset \mathcal{E}_{\rho}$; and P_{ρ_t} is identical to the global solution set in (2.1).

Alleviating the non-injectivity of the measurement map is a key step in formulating methods that guarantee exact recovery in phase retrieval literature [50], and offers us a blueprint in addressing (4). A key observation is that one can consider (5) as a mapping from a rank-1, positive semi-definite matrix $\rho \rho^H \in \mathbb{C}^{N \times N}$ instead of a quadratic map from the signal domain in \mathbb{C}^N , and attempt to recover $\rho_t \rho_t^H$. This approach is known as the *lifting* technique which is the main premise of LRMR based phase retrieval [35–37,51] and interferometric inversion methods [11,47,52].

2.2 Low Rank Matrix Recovery via Lifting

We adopt the concepts of the LRMR approach to the interferometric inversion problem based on PhaseLift [11], [36], and introduce the following definitions.

Definition 2.3. Lifting. Each correlated measurement in (2) can be written in the form of an inner product of two rank-1 operators, $\tilde{\rho}_t = \rho_t \rho_t^H$ and $\overline{\mathbf{F}}^m = \mathbf{L}_j^m (\mathbf{L}_i^m)^H$ such that¹

$$d_{ij}^{m} = \langle \mathbf{F}^{m}, \tilde{\boldsymbol{\rho}}_{t} \rangle \quad m = 1, ..., M$$
 (7)

where $\langle \cdot, \cdot \rangle$ is the Frobenius (or in infinite dimensions the Hilbert-Schmidt) inner product. We refer to the procedure of transforming interferometric inversion over \mathbb{C}^N (or phase retrieval for i = j) to the recovery of the rank-1 unknown $\tilde{\rho}_t$ in $\mathbb{C}^{N \times N}$ as lifting.

The lifting technique introduces a new linear measurement map which we define as follows:

Definition 2.4. Lifted Forward Model. Let $\mathbf{d} = [d_{ij}^1, d_{ij}^2, \cdots d_{ij}^M] \in \mathbb{C}^M$ denote the vector obtained from stacking the cross-correlated measurements in (2). Then, we define $\mathcal{F} : \mathbb{C}^{N \times N} \to \mathbb{C}^M$ in (7) as

$$\mathbf{d} = \mathcal{F}(\tilde{\boldsymbol{\rho}}_t) \tag{8}$$

and refer to \mathcal{F} as the lifted forward model or the lifted forward map.

Remark. The map \mathcal{F} can be interpreted as a $M \times N^2$ matrix with $\bar{\mathbf{F}}^m$ as its rows in the vectorized problem in which $N \times N$ variable $\tilde{\boldsymbol{\rho}}_t$ is concatenated into a vector.

We refer to the recovery of $\tilde{\rho}_t$ from **d** using the model (8) as the lifted problem, or interferometric inversion in the lifted domain.

The main advantage of lifting is that for all $\rho \in \mathbb{C}^N$, each non-convex equivalence set P_{ρ} is now mapped to a set with a single element $\tilde{\rho} = \rho \rho^H$. Using the definition of the lifted forward model, quadratic equality constraints reduce to affine equality constraints to define a convex manifold in $\mathbb{C}^{N \times N}$. From the rank-1 positive semi-definite (PSD) structure of the unknown $\tilde{\rho}_t$, interferometric inversion in the lifted domain corresponds to solving the following optimization problem:

find:
$$\mathbf{X}$$
 s.t. $\mathbf{d} = \mathcal{F}(\mathbf{X}), \ \mathbf{X} \succeq 0, \ \operatorname{rank}(\mathbf{X}) = 1.$ (9)

Here, we refer to $\mathbf{X} \in \mathbb{C}^{N \times N}$ as the lifted variable. Due to the fact that there surely exists a rank-1 solution from (8), (9) is equivalent to:

minimize: rank(
$$\mathbf{X}$$
) s.t. $\mathbf{d} = \mathcal{F}(\mathbf{X}), \ \mathbf{X} \succeq 0,$ (10)

which is known to be an NP-hard problem [53, 54]. Given its rank-minimization form, (10) is approached by low rank matrix recovery theory analogous to compressive sensing [55, 56]. Most prominently, the non-convex rank term of the objective function is relaxed by a convex surrogate, which under the positive semi-definite constraint, corresponds to the trace norm. This results in the following formulation [35, 36, 48]:

minimize: trace(
$$\mathbf{X}$$
) s.t. $\mathbf{d} = \mathcal{F}(\mathbf{X}), \ \mathbf{X} \succeq 0,$ (11)

 $^{^{1}(\}bar{\cdot})$ denotes element-wise complex conjugation

which can be solved in polynomial time via semi-definite programming. Alternatively, one can equivalently formulate the perturbed problem of (11) as

$$\underset{\mathbf{X} \succ 0}{\text{minimize:}} \frac{1}{2M} \| \mathcal{F}(\mathbf{X}) - \mathbf{d} \|_{2}^{2} + \lambda \operatorname{tr}(\mathbf{X}), \tag{12}$$

and solve it by Uzawa's method [53, 54], which is analogous to the singular value thresholding algorithm with a PSD constraint [11].

Notably, as $M \ll N^2$ in typical estimation problems, the lifted forward model has a non-trivial null space. LRMR theory encapsulates identifying necessary and sufficient conditions on \mathcal{F} in order to guarantee exact recovery despite having an under-determined system of equations in (8). The key conditions on \mathcal{F} are primarily characterized by its null space [57–59] or restricted isometry properties [54,60,61] on low rank matrices. Methods such as PhaseLift [35,36] and PhaseCut [37] assert conditions on the mapping \mathcal{F} such that there exists no feasible element in the PSD cone with a smaller trace than the true solution $\tilde{\rho_t}$, from which exact recovery results to a unique minimizer are directly implied by the standard arguments of semi-definite programming [36]. Furthermore, under the properties on \mathcal{F} asserted by PhaseLift, it is observed in [52] that the lifted problem can be robustly solved as a convex feasibility problem by Douglas-Rachford splitting by eliminating the trace minimization step completely.

Altogether, lifting based approaches provide a profound perspective to the interferometric inversion problem. Our observation is that the key principles of lifting based methods in establishing exact recovery guarantees are reciprocated in the WF framework. In fact, WF corresponds to solving a perturbed non-convex feasibility problem over the lifted domain, and in this sense, is reminiscent of the optimizationless PhaseLift method [52], and Uzawa's iterations [11]. To observe this, we introduce the GWF iterations for interferometric inversion, and develop the method as a solver in the lifted problem framework. The basis of our extension from WF to GWF framework is the identification of conditions on the lifted forward model for the uniqueness of a solution in the lifted domain.

2.3 GWF Iterations

In contrast to the lifting based approaches, the non-convex form of the problem in (4) is preserved in WF. Given an *accurate* initial estimate ρ_0 , WF involves using the following updates to refine the current estimate ρ_k :

$$\boldsymbol{\rho}_{k+1} = \boldsymbol{\rho}_k - \frac{\mu_{k+1}}{\|\boldsymbol{\rho}_0\|^2} \nabla \mathcal{J}(\boldsymbol{\rho}_k). \tag{13}$$

Notably, \mathcal{J} is a real-valued function of a complex variable $\boldsymbol{\rho} \in \mathbb{C}^N$, and therefore, non-holomorphic. Hence, the gradient over \mathcal{J} is defined by the means of Wirtinger derivatives

$$\nabla \mathcal{J} = \left(\frac{\partial \mathcal{J}}{\partial \boldsymbol{\rho}}\right)^H = \left(\frac{\partial \mathcal{J}}{\partial \overline{\boldsymbol{\rho}}}\right)^T, \text{ where}$$
(14)

$$\frac{\partial}{\partial \boldsymbol{\rho}} = \frac{1}{2} \left(\frac{\partial}{\partial \boldsymbol{\rho}_R} - i \frac{\partial}{\partial \boldsymbol{\rho}_I} \right), \quad \frac{\partial}{\partial \overline{\boldsymbol{\rho}}} = \frac{1}{2} \left(\frac{\partial}{\partial \boldsymbol{\rho}_R} + i \frac{\partial}{\partial \boldsymbol{\rho}_I} \right), \tag{15}$$

and $\rho = \rho_R + i\rho_I$, with $\rho_R, \rho_I \in \mathbb{R}^N$. Thus, the iterations in (13) correspond to that of the steepest descent method [1], where μ_{k+1} is the step size. For interferometric inversion by GWF,

 $\nabla \mathcal{J}$ evaluated at $\boldsymbol{\rho}_k$ is given by

$$\nabla \mathcal{J}(\boldsymbol{\rho}_k) = \frac{1}{2M} \sum_{m=1}^{M} \left[\overline{e_{ij}^m} (\mathbf{L}_j^m (\mathbf{L}_i^m)^H \boldsymbol{\rho}_k) + e_{ij}^m (\mathbf{L}_i^m (\mathbf{L}_j^m)^H \boldsymbol{\rho}_k) \right], \tag{16}$$

where $e_{ij}^m = ((\mathbf{L}_i^m)^H \boldsymbol{\rho}_k \boldsymbol{\rho}_k^H \mathbf{L}_j^m - d_{ij}^m)$ is the mismatch between the synthesized and cross-correlated measurements. See Appendix A.1 for the derivation of $\nabla \mathcal{J}$.

Note that for phase retrieval, we set i = j, $\mathbf{L}^m = \mathbf{L}_i^m = \mathbf{L}_j^m$ and $d^m = |\langle \mathbf{L}^m, \boldsymbol{\rho}_t \rangle|^2$, for $m = 1 \cdots M$, in which case (16) reduces to the standard WF iterations of [1].

An illuminating interpretation of the GWF update can be observed by examining (16) in the lifted problem. Moving the common term of the current iterate ρ_k outside the summation, (16) can be expressed as

$$\nabla \mathcal{J}(\boldsymbol{\rho}_k) = \frac{1}{M} \left[\frac{1}{2} \left(\sum_{m=1}^{M} \overline{e_{ij}^m} (\mathbf{L}_j^m (\mathbf{L}_i^m)^H) + \sum_{m=1}^{M} e_{ij}^m (\mathbf{L}_i^m (\mathbf{L}_j^m)^H) \right) \right] \boldsymbol{\rho}_k.$$
 (17)

Using the definition of the lifted forward model in (8), the second summation becomes the *back-projection* of the measurement error to the adjoint space of \mathcal{F} , which is defined as follows:

Definition 2.5. Backprojection. For the lifted forward model $\mathcal{F}: \mathbb{C}^{N \times N} \to \mathbb{C}^{M}$, we define the backprojection by the adjoint operator $\mathcal{F}^{H}: \mathbb{C}^{M} \to \mathbb{C}^{N \times N}$ of \mathcal{F} as follows:

$$\mathcal{F}^{H}(\mathbf{y}) = \sum_{m=1}^{M} y^{m} (\mathbf{L}_{i}^{m} \left(\mathbf{L}_{j}^{m}\right)^{H}). \tag{18}$$

where $\mathbf{y} = [y^1, y^2, \cdots y^M] \in \mathbb{C}^M$.

Since the averaged terms are Hermitian transposes of each other, the update term in (13) corresponds to backprojecting the mismatch between synthesized and true measurements, and then projecting it onto the set of symmetric matrices S, i.e.,

$$\nabla \mathcal{J}(\boldsymbol{\rho}_k) = \frac{1}{M} \mathcal{P}_S \left(\mathcal{F}^H(\mathbf{e}) \right) \boldsymbol{\rho}_k, \tag{19}$$

where $\mathbf{e} = [e_{ij}^1, e_{ij}^2, \cdots e_{ij}^M] \in \mathbb{C}^M$ is the measurement mismatch vector and $\mathcal{P}_S(\cdot)$ denotes the projection operator onto S.

The representation in (19) provides a novel perspective in interpreting GWF as a solver of the lifted problem. Consider the structure enforced by (13) for the non-relaxed form of the low rank recovery problem in (10). In the GWF updates, the rank of the lifted variable \mathbf{X} in (10) is fixed at one, and the rank minimization problem is converted to its original non-convex feasibility problem in (9). Knowing that (3) corresponds to the objective of the perturbed problem, the GWF solver of (3) can be equivalently cast as the solver of the following lifted problem:

minimize:
$$\frac{1}{2M} \| \mathcal{F}(\mathbf{X}) - \mathbf{d} \|_2^2$$
 s.t. $\operatorname{rank}(\mathbf{X}) = 1$ and $\mathbf{X} \succeq 0$. (20)

In lifting based approaches, we discussed Uzawa's method as a solver to the perturbed problem. Formulating Uzawa's iterations, a gradient step over the smooth ℓ_2 mismatch term is followed

by a projection onto the intersection of the PSD cone and the set of rank-1 matrices. While in general projections to the intersection of two sets is an optimization problem on its own, and the rank-1 constraint constitutes a non-convex manifold, there exists a simple projection for the set $\mathcal{X} = \{\mathbf{X} \in \mathbb{C}^{N \times N} : \operatorname{rank}(\mathbf{X}) = 1 \cap \mathbf{X} \succeq 0\}$ such that

$$\mathcal{P}_{\mathcal{X}} = \mathcal{P}_{r=1} \circ \mathcal{P}_{PSD},\tag{21}$$

which is the successive operation of the projection onto the PSD cone, followed by a rank-1 approximation.

WF framework offers an alternative formulation and update scheme to minimize the perturbed rank-1 recovery objective in (20). Observe that the rank-1 PSD constraint set precisely corresponds to the set of elements of $\mathcal{X} = \{ \boldsymbol{\rho} \boldsymbol{\rho}^H, \boldsymbol{\rho} \in \mathbb{C}^N \}$ as defined at the end of Section 2.1, and that (20) can be equivalently expressed as:

minimize:
$$\frac{1}{2M} \| \mathcal{F}(\mathbf{X}) - \mathbf{d} \|_2^2 \quad \text{s.t.} \quad \mathbf{X} = \boldsymbol{\rho} \boldsymbol{\rho}^H.$$
 (22)

The alternative update form stems from the fact PSD rank-1 constraint of the lifted unknown can be enforced by a variable transformation in the update equation, such that $\mathbf{X} = \rho \rho^H$, rather than projections by (21). The updates are thereby performed on the leading eigenspace of the lifted variable \mathbf{X} directly by means of the Jacobian $\frac{\partial \bar{\mathbf{X}}}{\partial \bar{\rho}}$. Having $\mathbf{X} = \mathbf{X}^H$, we obtain the updates²

$$\boldsymbol{\rho}_{k+1} = \boldsymbol{\rho}_k - \alpha_{k+1} \left(\frac{\partial \overline{\mathbf{X}}}{\partial \bar{\boldsymbol{\rho}}} \left(\frac{\partial \mathcal{J}}{\partial \overline{\mathbf{X}}} + \frac{\partial \mathcal{J}}{\partial \mathbf{X}} \right) \right)^T, \text{ where}$$
 (23)

$$\left(\frac{\partial \overline{\mathbf{X}}}{\partial \overline{\boldsymbol{\rho}}} \frac{\partial \ell}{\partial \overline{\mathbf{X}}}\right)^{T} = \frac{1}{2M} (\mathcal{F}^{H} \mathcal{F}(\mathbf{X}) - \mathcal{F}^{H} \mathbf{d}) \boldsymbol{\rho}, \quad \left(\frac{\partial \overline{\mathbf{X}}}{\partial \overline{\boldsymbol{\rho}}} \frac{\partial \ell}{\partial \mathbf{X}}\right)^{T} = \frac{1}{2M} (\mathcal{F}^{H} \mathcal{F}(\mathbf{X}) - \mathcal{F}^{H} \mathbf{d})^{H} \boldsymbol{\rho}. \tag{24}$$

Substituting $\mathbf{X} = \boldsymbol{\rho} \boldsymbol{\rho}^H$ in both terms in (23), and evaluating and adding them at iterate $\boldsymbol{\rho}_k$, gives precisely $\nabla \mathcal{J}(\boldsymbol{\rho}_k)$ derived in (19).

Clearly, the immediate advantage of the GWF formulation in (22) rather than the convex relaxations is the dimensionality reduction of the search space, attributed to iterating in the signal domain. There is yet another significant advantage to the GWF formulation regarding exact recovery. By (22), we formulate an iterative scheme for the unrelaxed, non-convex form of the lifted problem and enforce the rank-1 structure on the iterates. This allows the constraint set to be considerably *smaller* than that of the trace relaxation or the convex feasibility problems. Formally, the problem (22) has a unique solution if the equivalence set of any $\rho \in \mathbb{C}^N$ is its equivalence class under the correlation map \mathcal{L} as defined in Definition 2.2.

Condition 2.1. Uniqueness Condition. There exists a unique solution $\rho_t \rho_t^H \in \mathcal{X}$ for the problem in (22) if

$$P_{\rho} = \mathcal{E}_{\rho}, \quad \forall \rho \in \mathbb{C}^{N}.$$
 (25)

In other words, there should exist no element H in the null space of \mathcal{F} , such that $\rho_t \rho_t^H + H$ is a rank-1, PSD matrix. Therefore, for exact interferometric inversion by GWF, the null space

²We use the property of Wirtinger derivatives in writing the update (23), such that the derivative of a real valued function of a complex variable has the property that $(\frac{\partial \mathcal{J}}{\partial \mathbf{x}}) = (\frac{\partial \mathcal{J}}{\partial \overline{\mathbf{x}}})$

condition of the lifted forward model has to hold over a much less restrictive set than any of the approaches discussed in Section 2.2.

2.4 The Distance Metric

While the view of WF in the lifted problem and the formulation in (22) are illuminating, the algorithmic map of GWF operates exclusively on the signal domain in \mathbb{C}^N . The duality between the lifted domain and the signal domain is established by the distance metric of WF framework which is defined as follows [1]:

Definition 2.6. Let $\rho_t \in \mathbb{C}^N$ be an element of the global solution set in (2.1). The distance of an element $\rho \in \mathbb{C}^N$ to ρ_t is defined as [1]

$$\operatorname{dist}(\boldsymbol{\rho}, \boldsymbol{\rho}_t) = \|\boldsymbol{\rho} - e^{\mathrm{i}\phi(\boldsymbol{\rho})}\boldsymbol{\rho}_t\|, \text{ where } \phi(\boldsymbol{\rho}) := \underset{\phi \in [0, 2\pi]}{\operatorname{argmin}} \|\boldsymbol{\rho} - \boldsymbol{\rho}_t e^{\mathrm{i}\phi}\|.$$
 (26)

For the purpose of convergence, the metric implies that we are primarily interested in the distance of an estimate ρ to any of the elements in the non-convex solution set P. In technical terms, invoking Definition 2.2, (26) is a measure of distance between the equivalence sets P_{ρ} and P. By Definition 2.6, the ambiguity due to the invariance of the cross-correlation map, \mathcal{L} , to the global phase factors is evaded on \mathbb{C}^N , without lifting the problem. Observe that the phase ambiguity is indeed removed analytically, since the ℓ_2 norm is minimized when $\operatorname{Re}(\langle \rho, e^{i\Phi(\rho)} \rho_t \rangle) = |\langle \rho, \rho_t \rangle|$, which is achieved at $e^{i\Phi(\rho)} = \frac{\langle \rho_t, \rho \rangle}{|\langle \rho, \rho_t \rangle|}$. Hence, the squared distance becomes

$$\operatorname{dist}^{2}(\boldsymbol{\rho}, \boldsymbol{\rho}_{t}) = \|\boldsymbol{\rho}\|^{2} + \|\boldsymbol{\rho}_{t}\|^{2} - 2|\langle \boldsymbol{\rho}, \boldsymbol{\rho}_{t} \rangle|, \tag{27}$$

and is independent of any global phase factor on ρ or ρ_t . Geometrically, the metric suggests that the cosine of the angle θ between the elements ρ and ρ_t is given by

$$\cos \theta = \frac{|\langle \boldsymbol{\rho}, \boldsymbol{\rho}_t \rangle|}{\|\boldsymbol{\rho}\| \|\boldsymbol{\rho}_t\|},\tag{28}$$

which can be viewed as the angle between the subspaces spanned by the elements $\rho \rho^H$ and $\rho_t \rho_t^H$ in the lifted domain $\mathbb{C}^{N \times N}$. This can be seen by evaluating the error between the lifted terms as follows:

$$\|\boldsymbol{\rho}\boldsymbol{\rho}^{H} - \boldsymbol{\rho}_{t}\boldsymbol{\rho}_{t}^{H}\|_{F}^{2} = \|\boldsymbol{\rho}\boldsymbol{\rho}^{H}\|_{F}^{2} + \|\boldsymbol{\rho}_{t}\boldsymbol{\rho}_{t}^{H}\|_{F}^{2} - 2\operatorname{Re}(\langle\boldsymbol{\rho}\boldsymbol{\rho}^{H},\boldsymbol{\rho}_{t}\boldsymbol{\rho}_{t}^{H}\rangle_{F}), \tag{29}$$

where $\langle \cdot, \cdot \rangle_F$ denotes the Frobenius inner product. For two rank-1 arguments, the Frobenius inner product reduces to having $\operatorname{Re}(\langle \boldsymbol{\rho} \boldsymbol{\rho}^H, \boldsymbol{\rho}_t \boldsymbol{\rho}_t^H \rangle_F) = |\langle \boldsymbol{\rho}, \boldsymbol{\rho}_t \rangle|^2$, and the cosine of the angle between the elements becomes equal to $\cos^2(\theta)$. Since (28) is non-negative, the relationship between the two angles is one to one. Therefore, WF distance metric can be interpreted as a measure of distance between the lifted variables, and the convergence with respect to the metric (26) in signal domain is equivalent to convergence with respect to (29) in the lifted space.

2.5 Initialization via the Spectral Method

Having to solve a non-convex problem, exact recovery guarantees of the WF framework depend on the accuracy of the initial estimate ρ_0 . The initial estimate of the standard WF algorithm is computed by the spectral method which corresponds to the leading eigenvector of the following positive semi-definite matrix:

$$\mathbf{Y} = \frac{1}{M} \sum_{m=1}^{M} d^m \mathbf{L}^m (\mathbf{L}^m)^H, \tag{30}$$

where $\mathbf{L}^m = \mathbf{L}_i^m = \mathbf{L}_j^m$, and $d^m = |\langle \mathbf{L}^m, \boldsymbol{\rho}_t \rangle|^2$ for i = j. The leading eigenvector is scaled by the square root of the corresponding largest eigenvalue λ_0 of \mathbf{Y} . In [1], the spectral method is described from a stochastic perspective. By the strong law of large numbers, under the assumption that we have $\mathbf{L}^m \sim \mathcal{N}(0, \frac{1}{2}\mathbf{I}) + i\mathcal{N}(0, \frac{1}{2}\mathbf{I}), /m = 1, \dots, M$, the spectral matrix \mathbf{Y} becomes equal to

$$\mathbb{E}\left[\frac{1}{M}\sum_{m=1}^{M}d^{m}\mathbf{L}^{m}(\mathbf{L}^{m})^{H}\right] = \|\boldsymbol{\rho}_{t}\|^{2}\mathbf{I} + \boldsymbol{\rho}_{t}\boldsymbol{\rho}_{t}^{H},$$
(31)

as $M \to \infty$, which has the true solution ρ_t as its leading eigenvector. The concentration of the spectral matrix around its expectation is used to show that the leading eigenvector of **Y** is sufficiently accurate, such that the sequence of iterates $\{\rho_k\}$ of (13) converges to an element in the global solution set P.

In formulating the GWF framework, we view the spectral method as a procedure in the lifted domain. In fact, we observe that the spectral matrix of phase retrieval in (30) is the backprojection estimate of the lifted unknown $\tilde{\rho}_t = \rho_t \rho_t^H$. Having different measurement vectors \mathbf{L}_i^m and \mathbf{L}_j^m in the cross-correlated measurement case, using the definition of the backprojection operator in (18), we extend (30) and redefine \mathbf{Y} as follows:

$$\mathbf{Y} = \frac{1}{M} \mathcal{F}^{H}(\mathbf{d}) = \frac{1}{M} \sum_{m=1}^{M} d_{ij}^{m} \mathbf{L}_{i}^{m} \left(\mathbf{L}_{j}^{m} \right)^{H}.$$
(32)

As noted, the true solution $\tilde{\rho}_t = \rho_t \rho_t^H$ of the lifted problem lies in the positive semi-definite (PSD) cone. In standard WF for phase retrieval, the spectral matrix **Y** is formed by summation of positive semi-definite outer products that are scaled by \mathbb{R}^+ valued measurements $\{d^m\}_{m=1}^M$, as auto-correlations are by definition squared magnitudes. Hence, the WF spectral method generates an estimate of the lifted unknown within the constraint set by default. This obviously is not the case for the backprojection estimate (32) with the cross-correlated measurement model. Therefore, the extension of the spectral method to cross-correlations includes a projection step onto the PSD cone. Since the PSD cone is convex, its projection operator is non-expansive and yields a closer estimate to $\rho_t \rho_t^H$ than that of (32). The GWF spectral matrix then becomes

$$\hat{\mathbf{X}} := \frac{1}{2M} \sum_{m=1}^{M} d_{ij}^{m} \mathbf{L}_{i}^{m} \left(\mathbf{L}_{j}^{m} \right)^{H} + \overline{d_{ij}^{m}} \mathbf{L}_{j}^{m} \left(\mathbf{L}_{i}^{m} \right)^{H}.$$
(33)

We discard the positive semi-definitivity in (33), and only project onto the set of symmetric matrices, which is also convex. This is simply because only the leading eigenvector will be kept from the generated lifted estimate, which will be unaffected by the projection onto the PSD cone³. Letting λ_0 , \mathbf{v}_0 denote the leading eigenvalue-eigenvector pair of $\hat{\mathbf{X}}$, the GWF initial estimate $\boldsymbol{\rho}_0$ is

 $^{^{3}}$ Unless the leading eigenvalue is negative, a scenario that is excluded due to the conditions for exact recovery in Section 3.

determined as⁴

$$\boldsymbol{\rho}_0 = \sqrt{\lambda_0} \mathbf{v}_0. \tag{34}$$

Using the representation in the lifted problem in (32) and plugging in (8) for the measurements, the GWF spectral matrix $\hat{\mathbf{X}}$ can be written as

$$\hat{\mathbf{X}} := \frac{1}{M} \mathcal{P}_S \left(\mathcal{F}^H (\mathbf{d}) \right) = \frac{1}{M} \mathcal{P}_S \left(\mathcal{F}^H \mathcal{F} (\boldsymbol{\rho}_t \boldsymbol{\rho}_t^H) \right). \tag{35}$$

Hence, the leading eigenvalue-eigenvector extraction corresponds to keeping the rank-1, PSD approximation, $\tilde{\rho}_0 := \rho_0 \rho_0^H$, of the backprojection estimate in the lifted domain.

As a comparison, observe the LRMR approach for the interferometric inversion by PSD constrained singular value thresholding (SVT) algorithm [11]. Writing Uzawa's iterations for the lifted variable \mathbf{X} and Lagrange multipliers \mathbf{y} , starting from the initial point $\mathbf{y}^0 = 0$ we have

$$\mathbf{X}_k = \mathcal{P}_{\tau}(\mathcal{F}^H \mathbf{y}_{k-1}) \tag{36}$$

$$\mathbf{y}_k = \mathbf{y}_{k-1} + \alpha_k (\mathbf{d} - \mathcal{F}(\mathbf{X}_k)), \tag{37}$$

where α_k is the step size, subscript k denotes the iteration number and \mathcal{P}_{τ} is the shrinkage operator acting on the singular values of its argument with threshold $\tau = \alpha \lambda$, which through the multiplier λ of trace regularization, enforces the low-rank constraint.

It can be seen that the first full iteration of (36) produces the estimate $\hat{\mathbf{X}} = \mathcal{P}_{\tau}(\alpha_k \mathcal{F}^H \mathbf{d})$, which, prior to the singular value thresholding, is identical to the backprojection estimate computed by the spectral method. The spectral method simply differs from the first Uzawa iteration by keeping the rank-1, PSD approximation instead of the low-rank approximation. In other words, the spectral estimate is obtained by replacing the shrinkage operator \mathcal{P}_{τ} with the projection operator \mathcal{P}_{χ} defined in (21). As a result, the spectral method corresponds to the first Uzawa iteration to solve the perturbed non-convex rank-1 constrained problem in (20).

2.6 Computational Complexity

Compared to the LRMR approach, GWF provides significant reductions in computational complexity, and memory requirements. As shown in Section 2.5, GWF uses the first iteration of the Uzawa's method to compute an initial estimate ρ_0 , and replaces the following iterations over the lifted domain with iterations on the leading eigenspace. GWF requires the following operations at each iteration:

- 1. Computing and storing the linear terms $(\mathbf{L}_{i,j}^m)^H \boldsymbol{\rho}_k$, requiring M number of N multiplications for each, resulting in $\mathcal{O}(MN)$ multiplications.
- 2. Computing the error by cross correlating linear terms, requiring $\mathcal{O}(M)$ multiplications.
- 3. Multiplication of the linear terms $(\mathbf{L}_{i,j}^m)^H \boldsymbol{\rho}_k$ and the error e_{ij}^m for each $m=1,\cdots M$, requiring $\mathcal{O}(M)$ multiplications.
- 4. Multiplication of the result in 3 with vectors $\{\mathbf{L}_i^m\}_{m=1}^M$ and $\{\mathbf{L}_j^m\}_{m=1}^M$, requiring $\mathcal{O}(MN)$ multiplications.

⁴Note that (33) yields a symmetric matrix, hence have eigenvalues $\lambda_i \in \mathbb{R}$.

These operations result in $\mathcal{O}(MN)$ multiplications for each iteration. In comparison, initialization by spectral method consists of the outer product of the two measurement vectors for each of the M samples, resulting in $\mathcal{O}(MN^2)$ multiplications, followed by an eigenvalue decomposition with $\mathcal{O}(N^3)$ complexity. In conclusion, GWF offers significant savings for the computation cost of each iteration, as compared to LRMR given that $M \ll N^2$.

3 Exact Interferometric Inversion via GWF

In this section we present our exact recovery guarantees for interferometric inversion by GWF. Notably, we merge the exact recovery conditions of standard Wirtinger Flow that rely on statistical properties of the sampling vectors into a single condition on the lifted forward model. In Theorem 3.1, we state that if \mathcal{F} satisfies the restricted isometry property on the set of rank-1, positive semidefinite matrices with a sufficiently small restricted isometry constant, GWF is guaranteed to recover the true solution upto a global phase factor, for all $\rho_t \in \mathbb{C}^N$. Following Theorem 3.1, we establish the validity of our condition in Theorem 3.2 for the case of $\mathcal{O}(N \log N)$ measurements that are cross-correlations of i.i.d. complex Gaussian sampling vectors.

We begin by introducing the definitions of some concepts that appear in our theorem statements.

3.1 Preliminaries

Definition 3.1. ϵ -Neighborhood of P. We denote the ϵ -neighborhood of the global solution set P in (2.1) by $E(\epsilon)$ and define it as follows [1]:

$$E(\epsilon) = \{ \boldsymbol{\rho} \in \mathbb{C}^N : \operatorname{dist}(\boldsymbol{\rho}, P) \le \epsilon \}.$$
(38)

The set $E(\epsilon)$ is determined by the distance of the spectral initialization to the global solution set, i.e., $\epsilon = \operatorname{dist}(\boldsymbol{\rho}_0, \boldsymbol{\rho}_t)$. The main result of the standard WF framework is that, for Gaussian and coded diffraction pattern measurement models [1], ϵ is sufficiently small so that the objective function \mathcal{J} satisfies the following regularity condition:

Condition 3.1. Regularity Condition. The objective function \mathcal{J} satisfies the regularity condition if, for all $\rho \in E(\epsilon)$, the following holds

$$\operatorname{Re}\left(\langle \nabla \mathcal{J}(\boldsymbol{\rho}), (\boldsymbol{\rho} - \boldsymbol{\rho}_t e^{\mathrm{i}\phi(\boldsymbol{\rho})})\rangle\right) \ge \frac{1}{\alpha} \operatorname{dist}^2(\boldsymbol{\rho}, \boldsymbol{\rho}_t) + \frac{1}{\beta} \|\nabla \mathcal{J}(\boldsymbol{\rho})\|^2$$
(39)

for fixed $\alpha > 0$ and $\beta > 0$ such that $\alpha \beta > 4$.

The regularity condition guarantees that the iterations in (16) are contractions with respect to the distance metric (26), which ensures that all WF iterates remain in $E(\epsilon)$. Furthermore, from the definition of $\nabla \mathcal{J}$ in (16), the condition implies that there exists no $\rho \in E(\epsilon)$ that belongs to the equivalence class of ρ_t under the mapping \mathcal{L} . Hence, the uniqueness condition for exact recovery is satisfied locally, and 3.1 is a sufficient condition by Lemma 7.1 of [1] such that the algorithm iterates $\{\rho_k\}$ converge to P at a geometric rate. Overall, the spectral initialization is said to be sufficiently accurate, if (39) holds $\forall \rho \in E(\epsilon)$.

3.2 Sufficient Conditions For Exact Recovery

The condition we assert on the lifted forward model \mathcal{F} is the restricted isometry property on the set of rank-1, PSD matrices, \mathcal{X} .

Definition 3.2. Restricted Isometry Property (RIP). Let $\mathcal{A}: \mathbb{C}^{K \times N} \to \mathbb{C}^M$ denote a linear operator. Without loss of generality assume K < N. For every $1 \le r \le K$, the r – restricted isometry constant (RIC) is defined as the smallest $\delta_r < 1$ such that

$$(1 - \delta_r) \|\mathbf{X}\|_F^2 \le \|\mathcal{A}(\mathbf{X})\|^2 \le (1 + \delta_r) \|\mathbf{X}\|_F^2$$
(40)

holds for all matrices **X** of rank at most r, where $\|\mathbf{X}\|_F = \sqrt{\text{Tr}(\mathbf{X}^H \mathbf{X})}$ denotes the Frobenius norm.

Suppose (40) holds for all $\mathbf{X} \in \mathcal{X} \subset \mathbb{C}^{K \times N}$ that have rank-r with some constant $0 < \delta_{\mathcal{X},r} < 1$, then \mathcal{A} is said to satisfy the RIP-r on set \mathcal{X} with RIC- $\delta_{\mathcal{X},r}$. For the interferometric inversion problem, having K = N, if there exists $\delta_1 < 1$ such that \mathcal{F} in (8) satisfies the restricted isometry property on the PSD cone, we say that the lifted forward model satisfies the RIP-1 condition with RIC- $\delta_{\mathcal{X},1}$.

By its definition in (35), the accuracy of the spectral estimate fully hinges on the properties of the normal operator of the lifted problem, i.e., $\mathcal{F}^H \mathcal{F}$. (40) quantifies how close $\mathcal{F}^H \mathcal{F}$ is to an identity over its domain through the following lemma:

Lemma 3.1. Suppose \mathcal{F} satisfies the RIP-1 property with the RIC- δ . Let \mathcal{X} denote the set of rank-1 PSD matrices of size $N \times N$ such that $\mathcal{X} = \{\rho \rho^H : \rho \in \mathbb{C}^N\}$. Then, for any $\mathbf{X} \in \mathcal{X}$ we have

$$(\mathcal{F}^H \mathcal{F} - \mathbf{I})(\mathbf{X}) = \delta(\mathbf{X}) \tag{41}$$

where $\boldsymbol{\delta}: \mathcal{X} \to \mathbb{C}^M$ is a bounded operator such that

$$\|\boldsymbol{\delta}\| \leq \delta$$

with $\|\cdot\|$ being the spectral norm.

In the GWF framework, we identify RIP-1 as a sufficient condition for an arbitrary lifted forward model \mathcal{F} , which guarantees that the spectral initialization of GWF provides an initial estimate that is sufficiently accurate, i.e., GWF iterates are guaranteed to converge to a global solution in P starting from ρ_0 .

Theorem 3.1. Exact Recovery by GWF. Assume the lifted forward model \mathcal{F}^5 satisfies the RIP-1 condition with the restricted isometry constant (RIC)- δ_1 . Then, the initial estimate ρ_0 obtained from the spectral method by (33) and (34) satisfies

$$\operatorname{dist}^{2}(\boldsymbol{\rho}_{0}, \boldsymbol{\rho}_{t}) \leq \epsilon^{2} \|\boldsymbol{\rho}_{t}\|^{2}, \tag{42}$$

⁵With a normalization factor of $\frac{1}{\sqrt{M}}$, where M is the number of measurements.

where $\epsilon^2 = (2+\delta_1)(1-\sqrt{1-\frac{\delta_1}{1-\delta_1}})+\frac{\delta_1^2}{8}$, and the corresponding objective function $\mathcal{J}(\boldsymbol{\rho}) = \frac{1}{2}\|\mathcal{F}(\boldsymbol{\rho}\boldsymbol{\rho}^H) - \mathbf{d}\|_2^2$ of (3) satisfies the regularity condition (39).

Thus, for the iterations (16) with the fixed step size $\mu \leq \frac{2}{\beta}$, we have

$$\operatorname{dist}^{2}(\boldsymbol{\rho}_{k}, \boldsymbol{\rho}_{t}) \leq \epsilon^{2} (1 - \frac{2\mu}{\alpha})^{k} \|\boldsymbol{\rho}_{t}\|^{2}$$
(43)

such that
$$\frac{1}{\alpha} + \frac{c^2}{\beta} \leq (1 - \delta_2)(1 - \epsilon)(2 - \epsilon)$$
, where $\delta_2 = \frac{(2 + \epsilon)\delta_1}{\sqrt{(1 - \epsilon)(2 - \epsilon)}}$ and $c = (2 + \epsilon)(1 + \epsilon)(1 + \delta_2)$.

Proof. See Section 4.1.
$$\Box$$

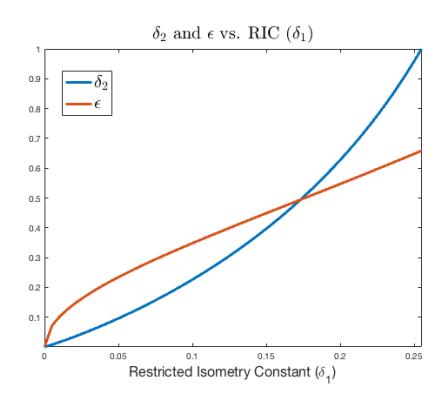
We refer to δ_2 as the restricted isometry constant of the *local* RIP-2 condition by Lemma 4.6, and c as the local Lipschitz constant of $\nabla \mathcal{J}$ by Lemma 4.7 both stated in Section 4.

Remark. We summarize the results of Theorem 3.1 by the following remarks.

- 1. Theorem 3.1 states the range of values the RIC- δ_1 can get. Clearly, the range of values for δ_1 is restricted because $\delta_2 < 1$ must hold. Numerically, plugging in the ϵ term defined by δ_1 , this condition is satisfied for $\delta_1 \leq 0.254$ as shown in Figure 1.
- 2. Notably, for any δ_1 in the valid region, the condition that $\alpha\beta > 4$ is directly implied since $\frac{1}{\alpha} + \frac{c^2}{\beta} < 1$ and $2 \le c$. Therefore, the RIP-1 condition for the lifted forward model with RIC- $\delta_1 \le 0.254$ is a sufficient condition for the exact recovery via GWF.
- 3. Theorem 3.1 indicates that the convergence speed of GWF algorithm is controlled by the restricted isometry constant δ_1 through c and δ_2 . As δ_1 approaches the critical limit of 0.254, c and δ_2 values increase super-linearly as shown in Figure 1. This has strong implications on the convergence speed, as β is inversely proportional to the step size μ , and quadratically related to the magnitude of c.
- 4. A notable consequence of our result is a universal upper bound on ϵ in the presence of the RIP-1 condition. As depicted in Figure 1, Theorem 3.1 defines what sufficiently close means numerically.

Remark. Despite solving the identical perturbed problem, GWF iterations provably converge, whereas the convergence guarantees of Uzawa's method vanish due to inclusion of a non-convex constraint. Similarly, the special structure of the constraint set and the GWF iterates suffice the RIP condition to be satisfied only over rank-1 matrices in the PSD cone, whereas the uniqueness condition of Uzawa's method requires RIP over the set of rank-2 matrices in the non-convex rank minimization problem.

Remark. The sufficient conditions of PhaseLift derived for semidefinite programming solvers for LRMR require ℓ_1 -restricted isometries on the PSD cone. In fact, the more stringent PhaseLift conditions directly imply the GWF sufficient condition when restricted on the set of rank-1, PSD matrices.



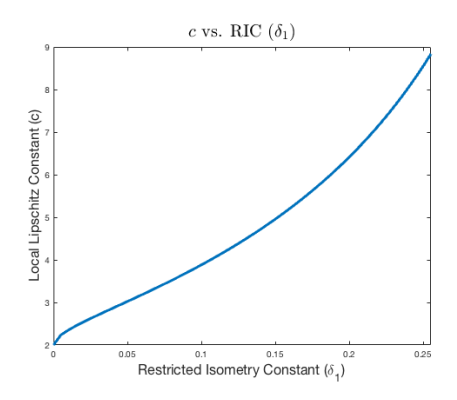


Figure 1: Numerical evaluation of ϵ , RIC- δ_2 and c values with respect to the RIC- $\delta_1 \leq 0.254$ of the restricted isometry property on the set of rank-1 PSD matrices.

3.3 Restricted Isometry Property for Cross-Correlation of Gaussian Measurements

Without loss of generality and following [1], we present the results for $\|\boldsymbol{\rho}_t\| = 1$. In standard WF for phase retrieval with the i.i.d. complex Gaussian model, i.e., $\mathbf{L}_m \sim \mathcal{N}(0, \mathbf{I}/2) + i\mathcal{N}(0, \mathbf{I}/2)$, the accuracy of the spectral estimate (30) is established as

$$\|\mathbf{Y} - (\boldsymbol{\rho}_t \boldsymbol{\rho}_t^H + \|\boldsymbol{\rho}_t\|^2 \mathbf{I})\| \le \delta \tag{44}$$

with probability $1 - 10e^{\gamma N} - 8/N^2$ where γ is a fixed positive numerical constant. This result is derived from the concentration bound of the Hessian of the objective function around its expectation at a global minimizer ρ_t such that

$$\|\nabla^2 \mathcal{J}(\boldsymbol{\rho}_t) - \mathbb{E}[\nabla^2 \mathcal{J}(\boldsymbol{\rho}_t)]\| \le \delta \tag{45}$$

where δ is the concentration bound.

In phase retrieval, plugging in the definition of phaseless measurements into (30), the autocorrelations yield the 4^{th} moments of the elements of the Gaussian measurement vectors. This introduces a bias of $\|\boldsymbol{\rho}_t\|^2 \mathbf{I}$ in the spectral estimate \mathbf{Y} as can be seen in (44). Moving from the autocorrelations to cross-correlations removes this bias component from the GWF spectral initialization. Hence, for the Gaussian model, cross-correlated measurement map satisfies the RIP-1 condition.

Theorem 3.2. RIP-1 Condition for Cross-Correlated Gaussian Measurements. Let the measurement vectors $\mathbf{L}_i^m, \mathbf{L}_j^m$ in (2) follow the i.i.d. complex Gaussian model, i.e. $\mathbf{L}_i^m, \mathbf{L}_j^m \sim \mathcal{N}(0, \mathbf{I}/2) + i\mathcal{N}(0, \mathbf{I}/2)$. Then, the lifted forward model \mathcal{F} in (8) for cross-correlated measurements, satisfies the RIP-1 property defined in (40) with probability $1 - 8e^{-\gamma N} - 5/N^2$ given $\mathcal{O}(N \log N)$ measurements, where γ is a fixed positive numerical constant. Moreover, the spectral matrix $\hat{\mathbf{X}}$ defined in (33) satisfies

$$\|\hat{\mathbf{X}} - \boldsymbol{\rho}_t \boldsymbol{\rho}_t^H\| \le \delta_1,\tag{46}$$

where ρ_t is the ground truth signal with $\|\rho_t\| = 1$ and δ_1 is the restricted isometry constant of \mathcal{F} .

Proof. See Section 4.2.
$$\Box$$

Remark. Theorem 3.2 establishes the relationship between the concentration bound of the spectral matrix, and the RIP-1 condition for interferometric inversion. This indicates that the regularity condition of WF framework is *redundant* for our problem if $\delta_1 \leq 0.254$, since by Theorem 3.1, RIP-1 condition directly implies the regularity condition.

Remark. Note that the equivalent linear model in the lifted domain actually has N^2 unknowns. By our formulation of GWF in the lifted problem, having measurements of the order of $N \log N$, therefore, corresponds to an under-determined system of equations in which exact recovery guarantees of GWF hold.

Remark. Note that our measurement complexity is identical to that of standard WF. This is an expected result, as the cross-correlations only impact the removal of the diagonal bias in the spectral matrix **Y**, not the concentration of **Y** around its expectation.

4 Proofs of Theorems 3.1 and 3.2

In this section, we present the proofs of Theorems 3.1 and 3.2. We first present key lemmas, and next prove the theorems using these lemmas. We provide the detailed proofs of the lemmas in Appendix B and C, respectively.

To prove Theorem 3.1, we begin by showing that the RIC- δ_1 of the RIP-1 condition determines the distance ϵ of the spectral initialization in a one-to-one manner. We then establish that the regularity condition is directly implied by the RIP-1 condition, for $\delta_1 \leq 0.254$. In achieving this result we first show that the structure of the rank-1 PSD set allows for restricted isometry property to hold locally for the difference of two rank-1 PSD matrices, i.e., a local RIP-2 condition similar to the one in [62], with a RIC- δ_2 . The upper bound on δ_1 ensures that RIC- δ_2 of the local RIP-2 satisfies $\delta_2 < 1$. The local RIP-2 condition, in turn, ensures that restricted strong convexity holds in the ϵ -neighborhood of the global solution set, which leads to exact recovery conditions of GWF.

For Theorem 3.2, we first show that the bias term in (44) resulting from the 4^{th} moments of the random Gaussian entries disappear when we have cross-correlations instead of auto-correlations of measurements. We then establish that the spectral matrix is concentrated around its expectation, using the machinery in [1], adapted for cross-correlations. Finally, we use the definition of the spectral matrix to derive the RIP-1 condition from the concentration bound, which yields the RIC- δ_1 .

4.1 Proof of Theorem 3.1

Without the loss of generality, we assume ρ_t is a solution with $\|\rho_t\| = 1$. In establishing the exact recovery guarantees for GWF, we take a two step approach. For a RIP-1 lifted forward map \mathcal{F} , we first show that the initialization by spectral method yields an estimate that is in the set $E(\epsilon)$. We then establish the regularity condition (39) for the objective function (3) in the ϵ -neighborhood defined by the initialization. These two results culminate into convergence to a global solution at a geometric rate as stated in Theorem 3.1.

Lemma 4.1. Assume that \mathcal{J} obeys the regularity condition for some fixed α, β for all $\rho \in E(\epsilon)$. Furthermore, let $\rho_0 \in E(\epsilon)$, and assume $\mu \leq 2/\beta$. Consider the following update

$$\boldsymbol{\rho}_{k+1} = \boldsymbol{\rho}_k - \mu \nabla \mathcal{J}(\boldsymbol{\rho}_k).$$

Then, for all k we have $\rho_k \in E(\epsilon)$ and

$$\operatorname{dist}^{2}(\boldsymbol{\rho}_{k}, \boldsymbol{\rho}_{t}) \leq (1 - \frac{2\mu}{\alpha})^{k} \operatorname{dist}^{2}(\boldsymbol{\rho}_{0}, \boldsymbol{\rho}_{t}).$$

Proof. See [1] Lemma 7.10.

Remark. As noted in [1] and defined in (13), μ is proportional to the squared norm of initial estimate, which is merely the leading eigenvalue λ_0 of the spectral matrix in (33). From Lemma 4.3, for a RIP-1 \mathcal{F} with the RIC- δ , λ_0 is lower bounded by $1 - \delta$, hence result of Lemma 4.1 for (13) holds for the values $\mu_k \leq (1 - \delta)\mu$.

4.1.1 ϵ -Neighborhood of Spectral Initialization

Rather than the law of large numbers approach in [1], we take the geometric point of view of [45] in establishing the ϵ -neighborhood of the spectral initialization. We begin by evaluating the distance of the leading eigenvector $\mathbf{v}_0 \in \mathbb{C}^N$ of the spectral matrix in (33) to the global solution set (2.1). Recall the definition of the distance metric

$$\operatorname{dist}(\mathbf{v}_0, \boldsymbol{\rho}_t) = \|\mathbf{v}_0 - e^{i\Phi(\mathbf{v}_0)} \boldsymbol{\rho}_t\| \tag{47}$$

which is essentially the Euclidean distance of \mathbf{v}_0 to the closest point in the solution set P in (2.1). Without loss of generality, we fix $\Phi(\mathbf{v}_0) = \Phi_0$ and incorporate it into ρ_t such that $\hat{\rho}_t = e^{i\Phi_0}\rho_t$ represents the closest solution to \mathbf{v}_0 in P. We breakdown the key arguments of our proof into the following three lemmas.

Lemma 4.2. Let ρ_t be a solution with $\|\rho_t\| = 1$ and $\hat{\rho}_t$ is the closest solution in P to \mathbf{v}_0 . Then, $\operatorname{Re}\langle \hat{\rho}_t, \mathbf{v}_0 \rangle = \langle \hat{\rho}_t, \mathbf{v}_0 \rangle$, and

$$\hat{\boldsymbol{\rho}}_t = \cos(\theta) \mathbf{v}_0 + \sin(\theta) \mathbf{v}_0^{\perp} \tag{48}$$

where $\|\mathbf{v}_0\| = 1$, $\cos(\theta) = \operatorname{Re}\langle \hat{\boldsymbol{\rho}}_t, \mathbf{v}_0 \rangle$, and \mathbf{v}_0^{\perp} is a unit vector lying in a plane whose normal is \mathbf{v}_0 . Similarly, there exists a perpendicular unit vector, $\hat{\boldsymbol{\rho}}_t^{\perp}$, to $\hat{\boldsymbol{\rho}}_t$ such that

$$\hat{\boldsymbol{\rho}}_t^{\perp} = -\sin(\theta)\mathbf{v}_0 + \cos(\theta)\mathbf{v}_0^{\perp}. \tag{49}$$

Proof. See Appendix B.1.

Lemma 4.3. Consider the spectral matrix $\hat{\mathbf{X}}$ given by (35), and denote the spectral matrix projected onto the positive semi-definite cone as $\hat{\mathbf{X}}_{PSD}$. Then, for the RIP-1 mapping \mathcal{F} with RIC- δ , $\hat{\mathbf{X}}$ and $\hat{\mathbf{X}}_{PSD}$ have the identical leading eigenvalue-eigenvector pair λ_0 , \mathbf{v}_0 such that

$$1 - \delta \le \lambda_0 \le 1 + \delta$$

and generate identical spectral initializations, ρ_0 .

Proof. See Appendix B.2.

Lemma 4.3 allows us to analyze the distance of the initial estimate ρ_0 to the solution set by the convenience either the positive semi-definite $\hat{\mathbf{X}}_{PSD}$ or the symmetric spectral estimate $\hat{\mathbf{X}}$, since they generate the same initial estimate ρ_0 .

Using the Lemmas 4.2 and 4.3 we reach the following key result.

Lemma 4.4. In the setup of Lemmas 4.2 and 4.3, for the angle θ between the one-dimensional sub-spaces spanned by $\hat{\rho}_t$ and \mathbf{v}_0 we have

$$\sin^2(\theta) \le \frac{\delta}{1 - \delta} \tag{50}$$

where δ is the RIC- δ_1 of the lifted map \mathcal{F} .

From Lemma 4.4, we can now lower bound the inner product of $\hat{\rho}_t$ and \mathbf{v}_0 such that

$$(\operatorname{Re}\langle \hat{\boldsymbol{\rho}}_t, \mathbf{v}_0 \rangle)^2 = \cos^2(\theta) = 1 - \sin^2(\theta) \ge 1 - \kappa,$$

where $\kappa = \frac{\delta}{1-\delta}$. Writing the distance of the spectral initialization $\rho_0 = \sqrt{\lambda_0} \mathbf{v}_0$ to the solution set, we have

$$dist^{2}(\boldsymbol{\rho}_{0}, \boldsymbol{\rho}_{t}) = \lambda_{0} + 1 - 2Re\langle e^{i\Phi(\boldsymbol{\rho}_{0})} \boldsymbol{\rho}_{t}, \sqrt{\lambda_{0}} \mathbf{v}_{0} \rangle.$$

It is easy to see that $\operatorname{Re}\langle e^{\mathrm{i}\Phi(\boldsymbol{\rho}_0)}\boldsymbol{\rho}_t,\sqrt{\lambda_0}\mathbf{v}_0\rangle$ is maximized when $\Phi(\boldsymbol{\rho}_0)=\Phi(\mathbf{v}_0)$, hence we get

$$\operatorname{dist}^{2}(\boldsymbol{\rho}_{0}, \boldsymbol{\rho}_{t}) = \lambda_{0} + 1 - 2\sqrt{\lambda_{0}}\operatorname{Re}\langle \hat{\boldsymbol{\rho}}_{t}, \mathbf{v}_{0}\rangle \leq \lambda_{0} + 1 - 2\sqrt{\lambda_{0}}\sqrt{1 - \kappa}.$$
 (51)

From Lemma 4.3, we know that $1 - \delta \le \lambda_0 \le 1 + \delta$. Moreover, the upper bound on the right hand side of (51) is simply a quadratic term with respect to $\sqrt{\lambda_0}$ since $\sqrt{\lambda_0}(\sqrt{\lambda_0} - 2\sqrt{1 - \kappa}) + 1$, which is maximized at the boundary of the domain of values $\sqrt{\lambda_0}$ takes. Since the quadratic equation is minimized at $\sqrt{1 - \kappa}$ and we have $1 - \kappa \le 1 - \delta$ for the domain of possible values of $0 \le \delta < 1$, $\lambda_0 = 1 + \delta$ is an upper bound for the right-hand-side of (51). Hence, we obtain

$$\operatorname{dist}^{2}(\boldsymbol{\rho}_{0}, \boldsymbol{\rho}_{t}) \leq 2 + \delta - 2\sqrt{1 + \delta}\sqrt{1 - \kappa}.$$

Writing the Taylor series expansion of $\sqrt{1+\delta}$ around 0, and discarding the components of order $\mathcal{O}(\delta^3)$ and higher, we have the final upper bound

$$\operatorname{dist}^{2}(\boldsymbol{\rho}_{0}, \boldsymbol{\rho}_{t}) \leq (2 + \delta)(1 - \sqrt{1 - \kappa}) + \frac{\delta^{2}}{8}, \tag{52}$$

which sets the ϵ -neighborhood as

$$\epsilon^2 = (2+\delta)(1-\sqrt{1-\kappa}) + \frac{\delta^2}{8}.\tag{53}$$

4.1.2 Proof of the Regularity Condition

Recall that we seek a solution to the interferometric inversion problem by minimizing the following loss function

$$\mathcal{J}(\boldsymbol{\rho}) = \frac{1}{2M} \sum_{m=1}^{M} |(\mathbf{L}_i^m)^H \boldsymbol{\rho} \boldsymbol{\rho}^H \mathbf{L}_j^m - d_m^{ij}|^2$$
(54)

and address it by forming the steepest descent iterates

$$\boldsymbol{\rho}^{k+1} = \boldsymbol{\rho}^k - \mu \nabla \mathcal{J}(\boldsymbol{\rho}^k), \tag{55}$$

where μ is the learning rate, and $\nabla \mathcal{J}$ is the complex gradient defined by the Wirtinger derivatives. As shown in Section 2.3, the gradient evaluated at a point ρ can be expressed as

$$\nabla \mathcal{J}(\boldsymbol{\rho}) = \mathcal{Y}(\boldsymbol{\rho})\boldsymbol{\rho},\tag{56}$$

where

$$\mathcal{Y}(\boldsymbol{\rho}) = \mathcal{P}_S \left(\mathcal{F}^H \mathcal{F}(\tilde{\boldsymbol{\rho}} - \tilde{\boldsymbol{\rho}}_t) \right) \tag{57}$$

with $\tilde{\rho}$ and $\tilde{\rho}_t$ denoting the lifted variables $\tilde{\rho} = \rho \rho^H$ and $\tilde{\rho}_t = \rho_t \rho_t^H$, respectively. Invoking Lemma 3.1 and the linearity of $\mathcal{F}^H \mathcal{F}$ and $\boldsymbol{\delta}$ of (41), (57) can be represented as

$$\mathcal{Y}(oldsymbol{
ho}) = \mathcal{P}_S \left(ilde{oldsymbol{
ho}} - ilde{oldsymbol{
ho}}_t + oldsymbol{\delta}(ilde{\mathbf{e}})
ight)$$

where $\tilde{\mathbf{e}} = \tilde{\rho} - \tilde{\rho}_t$ is the error in the lifted problem. Since the lifted variables are already symmetric we can take them out of the projection operator due its linearity. Hence, for the update term we obtain

$$\nabla \mathcal{J}(\boldsymbol{\rho}) = \mathcal{Y}(\boldsymbol{\rho})\boldsymbol{\rho} = \tilde{\boldsymbol{\rho}}\boldsymbol{\rho} - \tilde{\boldsymbol{\rho}}_t \boldsymbol{\rho} + \mathcal{P}_S(\boldsymbol{\delta}(\tilde{\mathbf{e}}))\boldsymbol{\rho}, \tag{58}$$

$$= \|\boldsymbol{\rho}\|^2 \boldsymbol{\rho} - (\boldsymbol{\rho}_t^H \boldsymbol{\rho}) \boldsymbol{\rho}_t + \mathcal{P}_S(\boldsymbol{\delta}(\tilde{\mathbf{e}})) \boldsymbol{\rho}. \tag{59}$$

Reprising the regularity condition under consideration, we need to establish that there exists constants α and β , such that $\alpha\beta > 4$ for all $\rho \in E(\epsilon)$ and

$$\operatorname{Re}\left(\langle \nabla \mathcal{J}(\boldsymbol{\rho}), (\boldsymbol{\rho} - \boldsymbol{\rho}_t e^{\mathrm{i}\phi(\boldsymbol{\rho})})\rangle\right) \ge \frac{1}{\alpha} \operatorname{dist}^2(\boldsymbol{\rho}, \boldsymbol{\rho}_t) + \frac{1}{\beta} \|\nabla \mathcal{J}(\boldsymbol{\rho})\|^2. \tag{60}$$

To show the existence of constants α and β that satisfy (60), we upper bound the gradient term, which converts the regularity condition to a restricted strong convexity condition [63,64]. We begin the proof by introducing the following key lemmas.

Lemma 4.5. Let ρ_t be the ground truth signal with $\|\rho_t\| = 1$, and $\hat{\rho}_t$ denote the global solution closest to ρ such that $\hat{\rho}_t = e^{i\Phi(\rho)}\rho_t$. Then, for any $\rho \in E(\epsilon)$, we have

$$(\sqrt{(1-\epsilon)(2-\epsilon)})\|\boldsymbol{\rho} - \hat{\boldsymbol{\rho}}_t\| \le \|\boldsymbol{\rho}\boldsymbol{\rho}^H - \boldsymbol{\rho}_t\boldsymbol{\rho}_t^H\|_F \le (2+\epsilon)\|\boldsymbol{\rho} - \hat{\boldsymbol{\rho}}_t\|.$$
(61)

Proof. See Appendix B.4.

Lemma 4.6. Let ρ_t be the ground truth signal with $\|\rho_t\| = 1$, and let the linear map \mathcal{F} satisfy the RIP-1 condition with RIC- δ_1 . Then, for $\delta_1 \leq 0.254$ and any $\rho \in E(\epsilon)$, we have $\delta_2 < 1$ such that

$$(1 - \delta_2) \| \boldsymbol{\rho} \boldsymbol{\rho}^H - \boldsymbol{\rho}_t \boldsymbol{\rho}_t^H \|_F^2 \le \| \mathcal{F} (\boldsymbol{\rho} \boldsymbol{\rho}^H - \boldsymbol{\rho}_t \boldsymbol{\rho}_t^H) \|^2 \le (1 + \delta_2) \| \boldsymbol{\rho} \boldsymbol{\rho}^H - \boldsymbol{\rho}_t \boldsymbol{\rho}_t^H \|_F^2, \tag{62}$$

where $\delta_2 = \frac{2+\epsilon}{\sqrt{(1-\epsilon)(2-\epsilon)}} \delta_1$.

We refer to (62) as the local RIP-2 condition in the lifted domain with RIC- δ_2 for the mapping \mathcal{F} . The two lemmas culminate into the local Lipschitz continuity of $\nabla \mathcal{J}$.

Proof. See Appendix B.5.
$$\Box$$

Lemma 4.7. In the setup of Lemmas 4.5 and 4.6, for any $\rho \in E(\epsilon)$, the objective function \mathcal{J} in (54) is Lipschitz differentiable with

$$\|\nabla \mathcal{J}(\boldsymbol{\rho})\| \le c \cdot \operatorname{dist}(\boldsymbol{\rho}, \boldsymbol{\rho}_t) \tag{63}$$

where $c = (1 + \epsilon)(2 + \epsilon)(1 + \delta_2)$ is the Lipschitz constant. Furthermore, to establish the regularity condition for \mathcal{J} , it is sufficient to show that

$$\operatorname{Re}\left(\langle \nabla \mathcal{J}(\boldsymbol{\rho}), (\boldsymbol{\rho} - \boldsymbol{\rho}_t e^{\mathrm{i}\phi(\boldsymbol{\rho})})\rangle\right) \ge \left(\frac{1}{\alpha} + \frac{c^2}{\beta}\right) \operatorname{dist}^2(\boldsymbol{\rho}, \boldsymbol{\rho}_t)$$
(64)

for any $\rho \in E(\epsilon)$.

Proof. See Appendix B.6.
$$\Box$$

We finally utilize the following lemma to obtain an alternative form of the restricted strong convexity condition [65].

Lemma 4.8. For the objective function \mathcal{J} in (54), the condition in (64) is satisfied if

$$\mathcal{J}(\boldsymbol{\rho}) \ge \frac{\eta}{2} \operatorname{dist}^2(\boldsymbol{\rho}, \boldsymbol{\rho}_t) \tag{65}$$

where $\eta = \frac{1}{\alpha} + \frac{c^2}{\beta}$.

Proof. See Appendix B.7.
$$\Box$$

Writing the objective function explicitly in terms of the lifted terms, and applying the lower bound from the RIP condition of the lifted forward model, we can express the regularity condition simply as

$$\frac{1}{2}\|\mathcal{F}[\boldsymbol{\rho}\boldsymbol{\rho}^H - \boldsymbol{\rho}_t\boldsymbol{\rho}_t^H]\|^2 \ge \frac{(1-\delta_2)}{2}\|\boldsymbol{\rho}\boldsymbol{\rho}^H - \boldsymbol{\rho}_t\boldsymbol{\rho}_t^H\|_F^2 \ge \frac{\eta}{2}\mathrm{dist}^2(\boldsymbol{\rho},\boldsymbol{\rho}_t),$$

where δ_2 is the restricted isometry constant for rank 2 matrices. From Lemma 4.5, the regularity condition is then satisfied by identifying α, β with $\alpha\beta > 4$ such that

$$\|\boldsymbol{\rho}\boldsymbol{\rho}^H - \boldsymbol{\rho}_t\boldsymbol{\rho}_t^H\|_F^2 \ge (1 - \delta_2)(1 - \epsilon)(2 - \epsilon)\mathrm{dist}^2(\boldsymbol{\rho}, \boldsymbol{\rho}_t) \ge (\frac{1}{\alpha} + \frac{c^2}{\beta})\mathrm{dist}^2(\boldsymbol{\rho}, \boldsymbol{\rho}_t),$$

where, from Lemma 4.7, $c = (1 + \epsilon)(2 + \epsilon)(1 + \delta_2)$.

4.2 Proof of Theorem 3.2

Lemma 4.9. Expectation of Spectral Matrix. Let measurement vectors $\mathbf{L}_i^m, \mathbf{L}_j^m$ be statistically independent and distributed according to the complex Gaussian model as $\mathbf{L}_i, \mathbf{L}_j^m \sim \mathcal{N}(0, \frac{1}{2}\mathbf{I}) + i\mathcal{N}(0, \frac{1}{2}\mathbf{I})$. Let $\boldsymbol{\rho}_t$ be independent of the measurement vectors, and \mathbf{Y} denote the backprojection estimate of the lifted signal generated by the spectral method, given as

$$\mathbf{Y} = \mathcal{F}^H \mathcal{F}(\boldsymbol{\rho}_t \boldsymbol{\rho}_t^H),$$

where \mathcal{F} is the lifted forward map in (8). Then,

$$\mathbb{E}[\mathbf{Y}] = \boldsymbol{\rho}_t \boldsymbol{\rho}_t^H.$$

Proof. See Appendix C.1.

Lemma 4.10. Concentration Around Expectation. In the setup of Lemma 4.9, assume that the number of measurements is as $M = C(\delta) \cdot N \log N$. Then,

$$\|\mathbf{Y} - \mathbb{E}[\mathbf{Y}]\| \le \delta$$

holds with probability at least $p = 1 - 8e^{-\gamma N} - 5N^{-2}$ where γ is a fixed positive constant.

Proof. See Appendix C.2.
$$\Box$$

Plugging in the expectation from Lemma 4.9, and using the definition of δ from Lemma 3.1, the Lemmas 4.9 and 4.10 culminate to

$$\|\boldsymbol{\delta}(\boldsymbol{\rho}_t \boldsymbol{\rho}_t^H)\| \le \delta, \tag{66}$$

for any ρ_t with $\|\rho_t\| = 1$ with probability at least p. From the definition of the spectral norm on $\mathbb{C}^{N\times N}$, we can write (66) equivalently as

$$\max_{\boldsymbol{\rho} \in C^N, \|\boldsymbol{\rho}\| = 1} |\boldsymbol{\rho}^H \boldsymbol{\delta}(\boldsymbol{\rho}_t \boldsymbol{\rho}_t^H) \boldsymbol{\rho}| \le \delta.$$
(67)

Since the spectral norm corresponds to the maximum over the unit sphere in \mathbb{C}^N , we have

$$|\boldsymbol{\rho}_t^H \boldsymbol{\delta}(\boldsymbol{\rho}_t \boldsymbol{\rho}_t^H) \boldsymbol{\rho}_t| \le \|\boldsymbol{\delta}(\boldsymbol{\rho}_t \boldsymbol{\rho}_t^H)\| \le \delta.$$
(68)

Observe that the left-hand-side can equivalently be represented as a Frobenius inner product via lifting as

$$|\boldsymbol{\rho}_t^H \boldsymbol{\delta}(\boldsymbol{\rho}_t \boldsymbol{\rho}_t^H) \boldsymbol{\rho}_t| = |\langle \boldsymbol{\delta}(\boldsymbol{\rho}_t \boldsymbol{\rho}_t^H), \boldsymbol{\rho}_t \boldsymbol{\rho}_t^H \rangle_F|.$$
(69)

Having Lemmas 4.9 and 4.10 hold for any element $\rho_t \in \mathbb{C}^N$ with $\|\rho_t\| = 1$ via unitary invariance, for any $\rho \in \mathbb{C}^N$ we obtain

$$\frac{\left|\langle (\mathcal{F}^H \mathcal{F} - \mathbf{I})(\boldsymbol{\rho} \boldsymbol{\rho}^H), \boldsymbol{\rho} \boldsymbol{\rho}^H \rangle_F \right|}{\|\boldsymbol{\rho} \boldsymbol{\rho}^H\|_F^2} \le \delta.$$
 (70)

Finally, invoking the Hermitian property of $\mathcal{F}^H \mathcal{F} - \mathbf{I}$ and extending the definition in [66], we get

$$(1 - \delta) \|\rho \rho^{H}\|_{F}^{2} \leq \|\mathcal{F}(\rho \rho^{H})\|^{2} \leq (1 + \delta) \|\rho \rho^{H}\|_{F}^{2}, \tag{71}$$

for any $\rho \in \mathbb{C}^N$. Therefore, the RIP-1 condition is established with probability at least p for mapping \mathcal{F} with $\mathbf{L}_i^m, \mathbf{L}_i^m \sim \mathcal{N}(0, \frac{1}{2}\mathbf{I}) + i\mathcal{N}(0, \frac{1}{2}\mathbf{I})$ where $M = C(\delta) \cdot N \log N$.

Furthermore, we know that the true lifted unknown $\rho_t \rho_t^H$ lies in the positive semi-definite cone, which is a convex set. Since the spectral matrix $\hat{\mathbf{X}}$ is the projection of $\mathcal{F}^H \mathcal{F}(\rho_t \rho_t^H)$ onto the set of Hermetian symmetric matrices, from the non-expansiveness property of projections onto convex sets we have

$$\|\hat{\mathbf{X}} - \boldsymbol{\rho}_t \boldsymbol{\rho}_t^H\| \le \|\mathcal{F}^H \mathcal{F}(\boldsymbol{\rho}_t \boldsymbol{\rho}_t^H) - \boldsymbol{\rho}_t \boldsymbol{\rho}_t^H\| \le \delta,$$

which completes the proof of Theorem 3.2.

5 Numerical Simulations

5.1 Signal Recovery From Random Gaussian Measurements

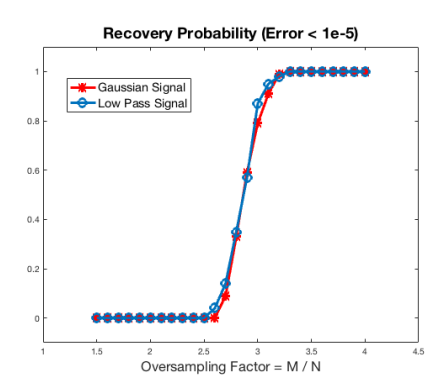
We begin by considering recovery of random signals from cross-correlations of complex random Gaussian measurements, $\mathbf{L}_i^m, \mathbf{L}_j^m \sim \mathcal{N}(\mathbf{0}, \frac{1}{2}\mathbf{I}) + \mathrm{i}\mathcal{N}(\mathbf{0}, \frac{1}{2}\mathbf{I})$. For our numerical evaluations of the Gaussian model, we conduct an experiment similar to that of [1]. We set N=128, and run 100 instances of interferometric inversion by GWF with independently sampled Gaussian measurement vectors on two types of signals: random low-pass signals, $\boldsymbol{\rho}^{LP}$, and random Gaussian signals, $\boldsymbol{\rho}^G$. The entries of the signals are generated independently of the measurement vectors at each instance by

$$\rho_l^{LP} = \sum_{p = -\frac{P}{2} + 1}^{\frac{P}{2}} (X_l + iY_l) e^{\frac{2\pi i(p-1)(l-1)}{N}}, \quad \rho_l^G = \sum_{p = -\frac{N}{2} + 1}^{\frac{N}{2}} \frac{1}{\sqrt{8}} (X_l + iY_l) e^{\frac{2\pi i(p-1)(l-1)}{N}}, \quad (72)$$

where P = N/8, and X_l and Y_l are i.i.d. $\mathcal{N}(0,1)$. As described in [1], random low-pass signal corresponds to a bandlimited version of this random model and variances are adjusted so that the expected signal power is the same.

We implement the GWF algorithm with the learning rate heuristic of WF in [1] such that the descent algorithm takes smaller steps initially due to higher inaccuracy of the iterates. The step size is gradually increased such that $\mu_k = \min(1 - e^{k/\tau_0}, \mu_{max})$, where $\tau_0 = 33000$, and $\mu_{max} = 0.2$. For 2500 iterations, the learning parameter corresponds to a nearly linear regime and attains the maximum value of 0.073.

In the experimentation, we compute the empirical probability of success after 2500 iterations by counting the exact recovery instances of GWF recovery from different realizations of Gaussian measurements for $\{\mathbf{L}_i^m, \mathbf{L}_j^m\}_{m=1}^M$. We evaluate the exact recovery by the relative normalized error of the final estimate, $\boldsymbol{\rho}_{GWF}$, such that $\mathrm{dist}(\boldsymbol{\rho}_{GWF}, \boldsymbol{\rho}_t)/\|\boldsymbol{\rho}_t\| \leq err = 10^{-5}$. In addition, we evaluate the probability of moderately precise recovery by setting $err = 10^{-3}$. As shown in Figure 2, our experimentation indicates that beginning with 3N interferometric Gaussian measurements, GWF achieves exact recovery with high probabilities. Furthermore, the method provides robust recovery with as low as 2.3N interferometric Gaussian measurements, with a relative error of 10^{-3} and below



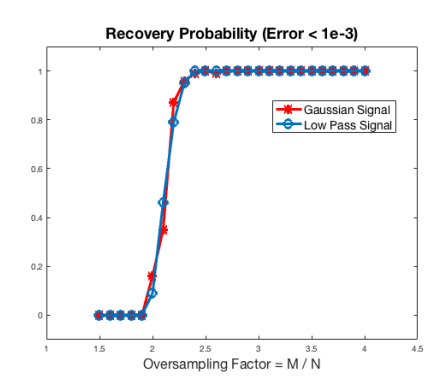


Figure 2: Empirical recovery probabilities based on 100 random trials vs. oversampling factor of the number of measurements M/N. The red curves correspond to empirical recovery probability of the Gaussian signal, whereas the blue curve corresponds to that of realization of the random low-pass signal model. The two figures vary with respect to the values of success criterion assumed for successful recovery, with a relative error of 10^{-5} and 10^{-3} , respectively.

at over 95 percent.

5.2 Multistatic Passive Radar Imaging

An interferometric inversion problem of great interest is multistatic passive radar imaging. We consider an imaging set-up in which several static, terrestrial receivers are placed in a circle of radius around the scene of interest, which is illuminated by a transmitter of opportunity. An exemplary multistatic imaging geometry is illustrated in Figure 3. At receiver i, the back-scattered signal is collected at a fixed location by a linear map \mathbf{L}_i parameterized by the temporal frequency variable ω . The linear measurements collected at two receivers i and j are then pairwise correlated in time to yield the cross-correlation model (2) defined in the temporal frequency domain.

The key advantage of the interferometric model is the elimination of the dependence of measurements on the transmitter location and phase of the transmitted waveform, both of which are unknown in the passive scenario. In prior studies, the interferometric wave-based imaging was approached by low rank recovery methods [11,12,67]. We postulate that GWF framework provides a computationally and memory-wise efficient alternative to LRMR based passive radar imaging.

5.2.1 Received Signal Model

Let $\mathbf{a}_i^r \in \mathbb{R}^3$ denote the spatial locations of the receivers, and assume S number of receivers such that $i = 1, 2, \dots S$. We assume that scattered signals are due to a single source of opportunity located at \mathbf{a}^t . The location on the surface of the earth is denoted by $\mathbf{x} = (\mathbf{x}, \psi(\mathbf{x})) \in \mathbb{R}^3$, where $\mathbf{x} = (x_1, x_2) \in \mathbb{R}^2$ and $\psi : \mathbb{R}^2 \to \mathbb{R}$ is a known ground topography; and $\rho : \mathbb{R}^2 \to \mathbb{R}$ denotes the ground reflectivity.

Under the flat topography assumption and Born approximation, and assuming waves propagate in free space, the fast-time temporal Fourier transform of the received signal at the i-th receiver can be modeled as [5]

$$f_i(\omega) \approx \mathcal{L}_i[\rho](\omega, s) := p(\omega, s) \int_D e^{-i\omega \frac{\phi_i(\mathbf{x})}{c_0}} \alpha_i(\mathbf{x}, \mathbf{a}^t) \rho(\mathbf{x}) d\mathbf{x},$$
 (73)

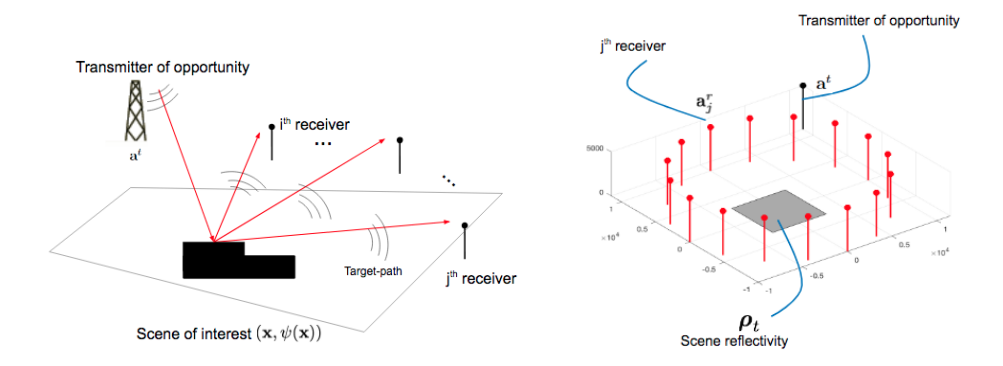


Figure 3: An illustration of a multistatic imaging configuration. A scene is illuminated by a stationary illuminator of opportunity, located at \mathbf{a}^t . The backscattered signal is measured by a collection of stationary receivers, encircling the scene of interest at locations \mathbf{a}_i^r .

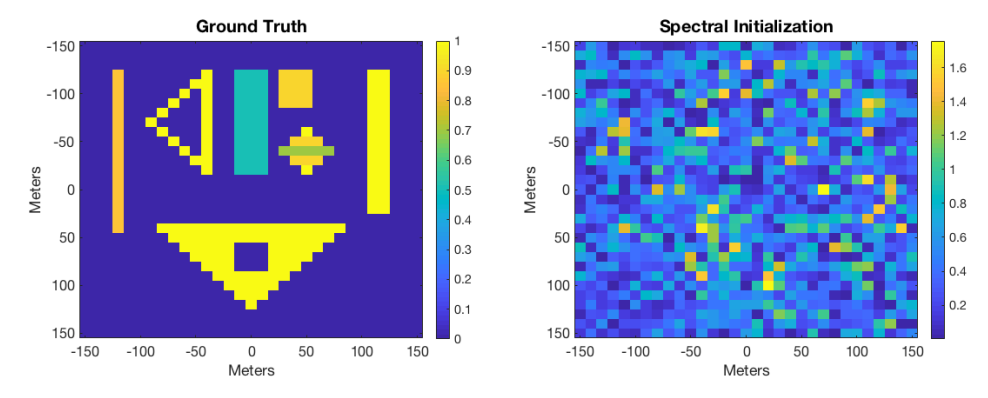


Figure 4: The ground truth image and the initial estimate by the spectral method of GWF by Equations (33) and (34).

where ω is the temporal frequency variable, c_0 is the speed-of-light in free space, $p(\omega, s)$ is the transmitted waveform, $\alpha_i(\mathbf{x}, \mathbf{a}^t)$ is the azimuth beam pattern, and

$$\phi_i(\mathbf{x}) = |\mathbf{x} - \mathbf{a}_i^r| + |\mathbf{x} - \mathbf{a}^t|, \tag{74}$$

is the bi-static delay term.

Following the derivations in [11] and discretizing the domain D of ρ into N samples, the cross-correlated data model for the multi-static scenario is obtained as

$$d_{ij}(\omega) = \sum_{k=1}^{N} e^{-i\omega(|\mathbf{x} - \mathbf{a}_i^r| + \hat{\mathbf{a}}^t \cdot \mathbf{x}_k)/c_0} \boldsymbol{\rho}_k \sum_{k'=1}^{N} e^{i\omega(|\mathbf{x}_{k'} - \mathbf{a}_j^r| + \hat{\mathbf{a}}^t \cdot \mathbf{x}_{k'})} \overline{\boldsymbol{\rho}_{k'}}$$
(75)

where $\rho_k = \rho(\mathbf{x}_k)$ is the k^{th} entry of the discretized scene reflectivity vector $\boldsymbol{\rho} \in \mathbb{C}^N$, and $\hat{\mathbf{a}}^t$ it the unit vector in the direction of the \mathbf{a}^t . We next discretize the temporal frequency domain Ω into O samples and define the measurement vectors with entries

$$[\mathbf{L}_i^m]_k = e^{\mathbf{i}\omega_m(|\mathbf{x}_k - \mathbf{a}_i^r| - \hat{\mathbf{a}}^t \cdot \mathbf{x}_k)/c_0} \quad k = 1, ..., N.$$

$$(76)$$

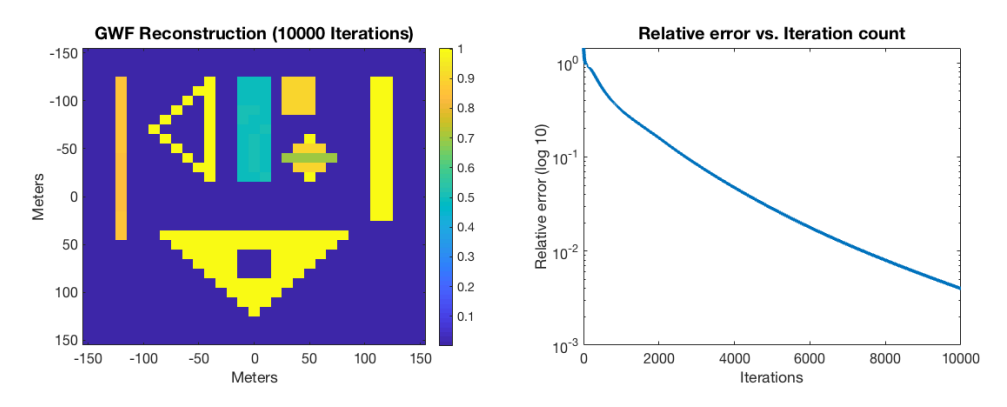


Figure 5: Reconstructed image by GWF after 10000 iterations of (13) and the relative error with respect to the ground truth in log-scale vs. iterations.

Rewriting (75) using (76), we obtain the interferometric measurement model as:

$$d^{ij}(\omega_o) = \langle \mathbf{L}_i^m, \, \boldsymbol{\rho} \rangle \overline{\langle \mathbf{L}_i^m, \, \boldsymbol{\rho} \rangle} \quad o = 1, ..., O, \ i = 1, ..., K, \ j \neq i, \tag{77}$$

which corresponds to total of $M\binom{S}{2}$ cross-correlated measurements. In [49], we show that the model in (75) satisfies the sufficient condition of Theorem 3.1, and hence GWF can provide exact image reconstruction for multi-static passive radar.

5.2.2 Simulation Setup and Results

We assume isotropic transmit and receive antennas, and simulate a transmitted signal with 20MHz bandwidth and 1GHz center frequency. We simulate a $300 \times 300 \text{m}^2$ scene, and discretize it by 10m, which corresponds to 31×31 pixels, hence, N = 961. We place the center of the scene at the origin of the coordinate system, and generate a phantom, which consists of multiple point and extended targets as depicted in Figure 4. The transmitter is fixed and located at coordinates $\mathbf{a}^t = [11.5, 11.5, 0.5]$ km. We simulate a flat spectrum waveform, and sample the temporal frequency domain into M = 32 samples. We use 16 receiver antennas that are placed in a circle of radius 10km around the scene at height of 0.5km, which corresponds to 120 unique cross-correlations at each temporal frequency sample.

We generate the back-scattered signals at each receiver by the linear measurement map of (73), and correlate linear measurements of the each pairwise combination of receivers to generate interferometric data. In reconstruction, we deploy the approximate measurement vectors in which the transmitter distance is removed as defined in (75) and (76), hence only the transmitter look-direction is used at recovery by GWF. In Figure 5, we demonstrate the reconstruction obtained by GWF after 10000 iterations, using the gradually increasing step size heuristic described in Section 5.1. In addition, we plot the relative error of GWF iterates, which displays a geometric rate of convergence as stated in Theorem 3.1. In comparison to traditional methods and LRMR approaches, results on our phantom image indicate GWF has the capacity to form accurate imagery of complex extended scenes.

6 Conclusion

In this paper, we present a novel framework for exact interferometric inversion. We approach the interferometric inversion problem from the perspective of phase retrieval techniques. We examine two of the most prominent phase retrieval methods, namely LRMR based PhaseLift, and non-convex optimization based WF, and bridge the theory between the two frameworks. We then generalize WF and formulate the GWF framework for interferometric inversion, and extend the exact recovery guarantees to arbitrary measurement maps with properties that are characterized in the equivalent lifted problem. Thereby, we establish exact recovery conditions for a larger class of problems than that of standard WF.

We identify the sufficient conditions for exact interferometric inversion on the lifted forward model as the restricted isometry property on rank-1, PSD matrices, with a restricted isometry constant of $\delta \leq 0.254$. In developing our theory, we use the special structure of the rank-1, PSD set of matrices to show that the RIP-1 condition directly implies the regularity condition of WF. Furthermore, we show that the concentration bound of the spectral matrix directly implies the RIP-1 condition for cross-correlations of the complex Gaussian model. Hence, generalizing the theory of WF for interferometric inversion in the complex Gaussian case, we demonstrate that the regularity condition becomes redundant. We illustrate that the empirical probability of exact interferometric inversion by GWF require smaller oversampling factors than that of phase retrieval in the Gaussian model. Finally, we demonstrate the applicability of GWF in a deterministic, passive multi-static radar imaging problem using realistic imaging parameters. In conclusion, our paper shows that the computational and theoretical advantages promote GWF as a practical technique in real-world imaging applications.

Acknowledgement

This work was supported by the Air Force Office of Scientific Research (AFOSR) under the agreement FA9550-16-1-0234, Office of Naval Research (ONR) under the agreement N0001418-1-2068 and by the National Science Foundation (NSF) under Grant No ECCS-1809234.

References

- [1] E. J. Candes, X. Li, and M. Soltanolkotabi, "Phase retrieval via wirtinger flow: Theory and algorithms," *IEEE Transactions on Information Theory*, vol. 61, no. 4, pp. 1985–2007, 2015.
- [2] R. M. Goldstein and H. Zebker, "Interferometric radar measurement of ocean surface currents," *Nature*, vol. 328, no. 6132, p. 707, 1987.
- [3] T. O. Saebo, "Seafloor depth estimation by means of interferometric synthetic aperture sonar," 2010.
- [4] R. Bamler and P. Hartl, "Synthetic aperture radar interferometry," *Inverse problems*, vol. 14, no. 4, p. R1, 1998.

- [5] C. Yarman and B. Yazici, "Synthetic aperture hitchhiker imaging," *IEEE Trans. Image Processing*, pp. 2156–2173, 2008.
- [6] L. Wang, C. Yarman, and B. Yazici, "Doppler-Hitchhiker: A novel passive synthetic aperture radar using ultranarrowband sources of opportunity," Geoscience and Remote Sensing, IEEE Trans., vol. 49, no. 10, pp. 3521–3537, Oct 2011.
- [7] L. Wang, I.-Y. Son, and B. Yazici, "Passive imaging using distributed apertures in multiple-scattering environments," *Inverse Problems*, vol. 26, no. 6, p. 065002, 2010.
- [8] C. E. Yarman, B. Yazici, and M. Cheney, "Bistatic synthetic aperture radar imaging for arbitrary flight trajectories," *IEEE Transactions on Image Processing*, vol. 17, no. 1, pp. 84– 93, 2008.
- [9] C. Yarman, L. Wang, and B. Yazici, "Doppler synthetic aperture hitchhiker imaging," *Inverse Problems*, vol. 26, no. 6, p. 065006, 2010. [Online]. Available: http://stacks.iop.org/0266-5611/26/i=6/a=065006
- [10] L. Wang and B. Yazici, "Bistatic synthetic aperture radar imaging using narrowband continuous waveforms," *Image Processing, IEEE Transactions on*, vol. 21, no. 8, pp. 3673–3686, Aug 2012.
- [11] E. Mason, I. Y. Son, and B. Yazıcı, "Passive synthetic aperture radar imaging using low-rank matrix recovery methods," *IEEE Journal of Selected Topics in Signal Processing*, vol. 9, no. 8, pp. 1570–1582, Dec 2015.
- [12] I.-Y. Son and B. Yazici, "Passive imaging with multistatic polarimetric radar," in *Radar Conference (RadarCon)*, 2015 IEEE. IEEE, 2015, pp. 1584–1589.
- [13] L. Wang and B. Yazici, "Ground moving target imaging using ultranarrowband continuous wave synthetic aperture radar," Geoscience and Remote Sensing, IEEE Trans., vol. 51, no. 9, pp. 4893–4910, Sept 2013.
- [14] —, "Bistatic synthetic aperture radar imaging of moving targets using ultra-narrowband continuous waveforms," SIAM Journal on Imaging Sciences, vol. 7, no. 2, pp. 824–866, 2014.
- [15] —, "Passive imaging of moving targets using sparse distributed apertures," SIAM Journal on Imaging Sciences, vol. 5, no. 3, pp. 769–808, 2012.
- [16] —, "Passive imaging of moving targets exploiting multiple scattering using sparse distributed apertures," *Inverse Problems*, vol. 28, no. 12, p. 125009, 2012.
- [17] I.-Y. Son and B. Yazici, "Passive polarimetric multistatic radar detection of moving targets," arXiv preprint arXiv:1706.09369, 2017.
- [18] S. Wacks and B. Yazici, "Passive synthetic aperture hitchhiker imaging of ground moving targets part 1: Image formation and velocity estimation," *IEEE Trans. Image Processing*, vol. 23, no. 6, pp. 2487–2500, June 2014.

- [19] —, "Passive synthetic aperture hitchhiker imaging of ground moving targets part 2: Performance analysis," *IEEE Trans. Image Processing*, vol. 23, no. 9, pp. 4126–4138, Sept 2014.
- [20] H. Ammari, J. Garnier, and W. Jing, "Passive array correlation-based imaging in a random waveguide," *Multiscale Modeling & Simulation*, vol. 11, no. 2, pp. 656–681, 2013.
- [21] T. S. Ralston, D. L. Marks, P. S. Carney, and S. A. Boppart, "Interferometric synthetic aperture microscopy," *Nature Physics*, vol. 3, no. 2, p. 129, 2007.
- [22] P. Stoica, J. Li, and Y. Xie, "On probing signal design for mimo radar," *IEEE Transactions on Signal Processing*, vol. 55, no. 8, pp. 4151–4161, 2007.
- [23] N. Patwari, J. N. Ash, S. Kyperountas, A. O. Hero, R. L. Moses, and N. S. Correal, "Locating the nodes: cooperative localization in wireless sensor networks," *IEEE Signal processing magazine*, vol. 22, no. 4, pp. 54–69, 2005.
- [24] S. Gezici, Z. Tian, G. B. Giannakis, H. Kobayashi, A. F. Molisch, H. V. Poor, and Z. Sahinoglu, "Localization via ultra-wideband radios: a look at positioning aspects for future sensor networks," *IEEE signal processing magazine*, vol. 22, no. 4, pp. 70–84, 2005.
- [25] J. E. Guivant and E. M. Nebot, "Optimization of the simultaneous localization and mapbuilding algorithm for real-time implementation," *IEEE transactions on robotics and automa*tion, vol. 17, no. 3, pp. 242–257, 2001.
- [26] J. Garnier, "Imaging in randomly layered media by cross-correlating noisy signals," *Multiscale Modeling & Simulation*, vol. 4, no. 2, pp. 610–640, 2005.
- [27] O. I. Lobkis and R. L. Weaver, "On the emergence of the greens function in the correlations of a diffuse field," The Journal of the Acoustical Society of America, vol. 110, no. 6, pp. 3011–3017, 2001.
- [28] P. Blomgren, G. Papanicolaou, and H. Zhao, "Super-resolution in time-reversal acoustics," *The Journal of the Acoustical Society of America*, vol. 111, no. 1, pp. 230–248, 2002.
- [29] P. Gough and M. Miller, "Displaced ping imaging autofocus for a multi-hydrophone sas," *IEE Proceedings-Radar, Sonar and Navigation*, vol. 151, no. 3, pp. 163–170, 2004.
- [30] S. Flax and M. O'Donnell, "Phase-aberration correction using signals from point reflectors and diffuse scatterers: Basic principles," *IEEE transactions on ultrasonics, ferroelectrics, and frequency control*, vol. 35, no. 6, pp. 758–767, 1988.
- [31] E. Mason and B. Yazici, "Robustness of lrmr based passive radar imaging to phase errors," in *EUSAR 2016: 11th European Conference on Synthetic Aperture Radar, Proceedings of.* VDE, 2016, pp. 1–4.
- [32] B. Jain and A. Taylor, "Cross-correlation tomography: measuring dark energy evolution with weak lensing," *Physical Review Letters*, vol. 91, no. 14, p. 141302, 2003.
- [33] E. J. Copeland, M. Sami, and S. Tsujikawa, "Dynamics of dark energy," *International Journal of Modern Physics D*, vol. 15, no. 11, pp. 1753–1935, 2006.

- [34] J. C. Schotland, "Quantum imaging and inverse scattering," *Optics letters*, vol. 35, no. 20, pp. 3309–3311, 2010.
- [35] E. Candes, Y. Eldar, T. Strohmer, and V. Voroninski, "Phase retrieval via matrix completion," SIAM Journal on Imaging Sciences, vol. 6, no. 1, pp. 199–225, 2013.
- [36] E. Candes and T. Strohmer, "Phaselift: Exact and stable recovery from magnitude measurements via convex programming," Comm Pure Appl Math, vol. 66, pp. 1241–1274, 2013.
- [37] I. Waldspurger, A. d'Aspremont, and S. Mallat, "Phase recovery, maxcut and complex semidefinite programming," *Mathematical Programming*, vol. 149, no. 1, pp. 47–81, 2015. [Online]. Available: http://dx.doi.org/10.1007/s10107-013-0738-9
- [38] T. Bendory, Y. C. Eldar, and N. Boumal, "Non-convex phase retrieval from stft measurements," *IEEE Transactions on Information Theory*, vol. 64, no. 1, pp. 467–484, 2018.
- [39] Y. Chen and E. Candes, "Solving random quadratic systems of equations is nearly as easy as solving linear systems," in *Advances in Neural Information Processing Systems*, 2015, pp. 739–747.
- [40] J. Chen, L. Wang, X. Zhang, and Q. Gu, "Robust wirtinger flow for phase retrieval with arbitrary corruption," arXiv preprint arXiv:1704.06256, 2017.
- [41] H. Zhang, Y. Chi, and Y. Liang, "Median-truncated nonconvex approach for phase retrieval with outliers," 2017, preprint.
- [42] H. Zhang and Y. Liang, "Reshaped wirtinger flow for solving quadratic systems of equations," stat, vol. 1050, p. 25, 2016.
- [43] R. Kolte and A. Özgür, "Phase retrieval via incremental truncated wirtinger flow," arXiv preprint arXiv:1606.03196, 2016.
- [44] H. Zhang, Y. Zhou, Y. Liang, and Y. Chi, "Reshaped wirtinger flow and incremental algorithms for solving quadratic systems of equations," 2017, preprint.
- [45] G. Wang, G. B. Giannakis, and Y. C. Eldar, "Solving systems of random quadratic equations via truncated amplitude flow," *IEEE Transactions on Information Theory*, vol. 64, no. 2, pp. 773–794, 2018.
- [46] S. Wacks *et al.*, "Doppler-dpca and doppler-ati: novel sar modalities for imaging of moving targets using ultra-narrowband waveforms," *IEEE Transactions on Computational Imaging*, vol. 4, no. 1, pp. 125–136, 2018.
- [47] L. Demanet and V. Jugnon, "Convex recovery from interferometric measurements." CoRR, vol. abs/1307.6864, 2013. [Online]. Available: http://dblp.uni-trier.de/db/journals/corr/corr1307.html
- [48] A. Chai, M. Moscoso, and G. Papanicolaou, "Array imaging using intensity-only measurements," *Inverse Problems*, vol. 27, no. 1, p. 015005, 2011. [Online]. Available: http://stacks.iop.org/0266-5611/27/i=1/a=015005

- [49] I. Y. Son, B. Yonel, and B. Yazici, "Supplement: Rip-1 condition for distributed multi-static radar," 2019.
- [50] A. S. Bandeira, J. Cahill, D. G. Mixon, and A. A. Nelson, "Saving phase: Injectivity and stability for phase retrieval," *Applied and Computational Harmonic Analysis*, vol. 37, no. 1, pp. 106–125, 2014.
- [51] E. J. Candes, X. Li, and M. Soltanolkotabi, "Phase retrieval from coded diffraction patterns," *Applied and Computational Harmonic Analysis*, vol. 39, no. 2, pp. 277–299, 2015.
- [52] L. Demanet and P. Hand, "Stable optimizationless recovery from phaseless linear measurements," *Journal of Fourier Analysis and Applications*, vol. 20, no. 1, pp. 199–221, 2014. [Online]. Available: http://dx.doi.org/10.1007/s00041-013-9305-2
- [53] J.-F. Cai, E. J. Candès, and Z. Shen, "A singular value thresholding algorithm for matrix completion," SIAM Journal on Optimization, vol. 20, no. 4, pp. 1956–1982, 2010.
- [54] B. Recht, M. Fazel, and P. A. Parrilo, "Guaranteed minimum-rank solutions of linear matrix equations via nuclear norm minimization," *SIAM review*, vol. 52, no. 3, pp. 471–501, 2010.
- [55] D. L. Donoho, "Compressed sensing," *IEEE Transactions on information theory*, vol. 52, no. 4, pp. 1289–1306, 2006.
- [56] E. J. Candes, J. K. Romberg, and T. Tao, "Stable signal recovery from incomplete and inaccurate measurements," Communications on Pure and Applied Mathematics: A Journal Issued by the Courant Institute of Mathematical Sciences, vol. 59, no. 8, pp. 1207–1223, 2006.
- [57] B. Recht, W. Xu, and B. Hassibi, "Necessary and sufficient conditions for success of the nuclear norm heuristic for rank minimization," in *Decision and Control*, 2008. CDC 2008. 47th IEEE Conference on. IEEE, 2008, pp. 3065–3070.
- [58] —, "Null space conditions and thresholds for rank minimization," *Mathematical programming*, vol. 127, no. 1, pp. 175–202, 2011.
- [59] S. Oymak, K. Mohan, M. Fazel, and B. Hassibi, "A simplified approach to recovery conditions for low rank matrices," in *Information Theory Proceedings (ISIT)*, 2011 IEEE International Symposium on. IEEE, 2011, pp. 2318–2322.
- [60] T. T. Cai, "Sharp rip bound for sparse signal and low-rank matrix recovery," Appl. Comput. Harmon. Anal, vol. 35, pp. 74–93, 2013.
- [61] S. Bhojanapalli, B. Neyshabur, and N. Srebro, "Global optimality of local search for low rank matrix recovery," in *Advances in Neural Information Processing Systems*, 2016, pp. 3873–3881.
- [62] X. Li, S. Ling, T. Strohmer, and K. Wei, "Rapid, robust, and reliable blind deconvolution via nonconvex optimization," *Applied and Computational Harmonic Analysis*, 2018.
- [63] Y. Chen and E. J. Candes, "Solving random quadratic systems of equations is nearly as easy as solving linear systems," Communications on Pure and Applied Mathematics, vol. 70, pp. 0822–0883, 2017.

- [64] J. Sun, Q. Qu, and J. Wright, "A geometric analysis of phase retrieval," Foundations of Computational Mathematics, vol. 18, no. 5, pp. 1131–1198, 2018.
- [65] H. Zhang and L. Cheng, "Restricted strong convexity and its applications to convergence analysis of gradient-type methods in convex optimization," *Optimization Letters*, vol. 9, no. 5, pp. 961–979, 2015.
- [66] S. Foucart and H. Rauhut, A mathematical introduction to compressive sensing. Birkhäuser Basel, 2013, vol. 1, no. 3.
- [67] B. Yonel, I.-Y. Son, and B. Yazici, "Generalized wirtinger flow for passive polarimetric reconstruction of extended dipole targets," in 2018 IEEE Radar Conference (RadarConf18). IEEE, 2018, pp. 1353–1358.
- [68] R. Vershynin, "Introduction to the non-asymptotic analysis of random matrices," arXiv preprint arXiv:1011.3027, 2010.

A Derivations

A.1 Derivation of $\nabla \mathcal{J}$

Recall the objective function \mathcal{J} in (3)

$$\mathcal{J}(\boldsymbol{\rho}) = \frac{1}{2M} \sum_{m=1}^{M} | (\mathbf{L}_i^m)^H \boldsymbol{\rho} \boldsymbol{\rho}^H \mathbf{L}_j^m - d_m^{ij} |^2.$$
 (78)

Letting $e_m = (\mathbf{L}_i^m)^H \boldsymbol{\rho} \boldsymbol{\rho}^H \mathbf{L}_i^m - d_m^{ij}$, we write

$$\frac{\partial \mathcal{J}}{\partial \boldsymbol{\rho}} = \frac{1}{2M} \sum_{m=1}^{M} \frac{\partial}{\partial \boldsymbol{\rho}} (e_m \bar{e}_m) = \frac{1}{2M} \sum_{m=1}^{M} \frac{\partial e_m}{\partial \boldsymbol{\rho}} \bar{e}_m + \frac{\partial \bar{e}_m}{\partial \boldsymbol{\rho}} e_m. \tag{79}$$

Having ρ and ρ^H independent by properties of Wirtinger derivatives, we compute the partial derivatives in (79) as

$$\frac{\partial \mathcal{J}}{\partial \boldsymbol{\rho}} = \frac{1}{2M} \sum_{m=1}^{M} \bar{e}_m(\boldsymbol{\rho}^H \mathbf{L}_j^m (\mathbf{L}_i^m)^H) + e_m(\boldsymbol{\rho}^H \mathbf{L}_i^m (\mathbf{L}_j^m)^H). \tag{80}$$

Using the definition of complex gradient provided in (14), we finally get

$$\nabla \mathcal{J} = \frac{1}{2M} \sum_{m=1}^{M} \bar{e}_{m} \mathbf{L}_{j}^{m} \left(\mathbf{L}_{i}^{m}\right)^{H} \boldsymbol{\rho} + e_{m} \mathbf{L}_{i}^{m} \left(\mathbf{L}_{j}^{m}\right)^{H} \boldsymbol{\rho}. \tag{81}$$

A.2 Proof Of Lemma 3.1

Assuming the RIP-1 condition with RIC- δ on \mathcal{F} , denoting $\tilde{\rho} = \rho \rho^H$ we write

$$(1 - \delta) \|\tilde{\rho}\|_F^2 \le \|\mathcal{F}(\tilde{\rho})\|^2 \le (1 + \delta) \|\tilde{\rho}\|_F^2. \tag{82}$$

Equivalently, from the definition of the Frobenius inner product and the adjoint operator \mathcal{F}^H , we re-express (82) as

$$(1 - \delta)\langle \tilde{\boldsymbol{\rho}}, \tilde{\boldsymbol{\rho}} \rangle_F \le \langle \mathcal{F}^H \mathcal{F}(\tilde{\boldsymbol{\rho}}), \tilde{\boldsymbol{\rho}} \rangle_F \le (1 + \delta)\langle \tilde{\boldsymbol{\rho}}, \tilde{\boldsymbol{\rho}} \rangle_F, \tag{83}$$

$$|\langle (\mathcal{F}^H \mathcal{F} - \mathbf{I})(\tilde{\boldsymbol{\rho}}), \tilde{\boldsymbol{\rho}} \rangle_F| \leq \delta \|\tilde{\boldsymbol{\rho}}\|_F^2,$$
 (84)

for all $\rho \in \mathbb{C}^N$. Since $\mathcal{F}^H \mathcal{F} - \mathbf{I} : \mathcal{X} \to \mathbb{C}^M$ is Hermitian, by Definition 6.1 in [66], we have

$$\max_{\boldsymbol{\rho} \in \mathbb{C}^N \setminus \{0\}} \frac{\left| \langle (\mathcal{F}^H \mathcal{F} - \mathbf{I})(\tilde{\boldsymbol{\rho}}), \tilde{\boldsymbol{\rho}} \rangle_F \right|}{\|\tilde{\boldsymbol{\rho}}\|_F^2} = \|\mathcal{F}^H \mathcal{F} - \mathbf{I}\| \le \delta.$$
 (85)

B Lemmas for Theorem 3.1

B.1 Proof of Lemma 4.2

Since $\hat{\boldsymbol{\rho}}_t = e^{\mathrm{i}\Phi(\mathbf{v}_0)}\boldsymbol{\rho}_t$, we have

$$dist^{2}(\mathbf{v}_{0}, \boldsymbol{\rho}_{t}) = \|\mathbf{v}_{0} - \hat{\boldsymbol{\rho}}_{t}\|^{2} = \|\mathbf{v}_{0}\|^{2} + \|\hat{\boldsymbol{\rho}}_{t}\|^{2} - 2\operatorname{Re}\langle\hat{\boldsymbol{\rho}}_{t}, \mathbf{v}_{0}\rangle, \tag{86}$$

Knowing that $\Phi(\mathbf{v}_0)$ achieves $\operatorname{Re}\langle \hat{\boldsymbol{\rho}}_t, \mathbf{v}_0 \rangle = |\langle \boldsymbol{\rho}_t, \mathbf{v}_0 \rangle|$, we have

$$\operatorname{Re}\langle \hat{\boldsymbol{\rho}}_t, \mathbf{v}_0 \rangle = \langle \hat{\boldsymbol{\rho}}_t, \mathbf{v}_0 \rangle = |\langle e^{i\Phi(\mathbf{v}_0)} \boldsymbol{\rho}_t, \mathbf{v}_0 \rangle|.$$
 (87)

Since $\hat{\rho}_t$ and \mathbf{v}_0 are unit norm, the geometric angle between them can be written as

$$\cos(\theta) = \langle \hat{\boldsymbol{\rho}}_t, \mathbf{v}_0 \rangle. \tag{88}$$

Invoking the representation theorem in Hilbert spaces, there exists a unit vector \mathbf{v}_0^{\perp} that lies in the plane whose normal is \mathbf{v}_0 such that

$$\langle \hat{\boldsymbol{\rho}}_t, \mathbf{v}_0 \rangle = \cos(\theta) \langle \mathbf{v}_0, \mathbf{v}_0 \rangle + \sin(\theta) \langle \mathbf{v}_0^{\perp}, \mathbf{v}_0 \rangle,$$
 (89)

$$\langle \hat{\boldsymbol{\rho}}_t - (\cos(\theta)\mathbf{v}_0 + \sin(\theta)\mathbf{v}_0^{\perp}), \mathbf{v}_0 \rangle = 0.$$
 (90)

The inner product is zero only when: 1) $\hat{\boldsymbol{\rho}}_t = \cos(\theta)\mathbf{v}_0 + \sin(\theta)\mathbf{v}_0^{\perp}$, 2) $\hat{\boldsymbol{\rho}}_t - (\cos(\theta)\mathbf{v}_0 + \sin(\theta)\mathbf{v}_0^{\perp})$ is perpendicular to \mathbf{v}_0 . The latter case occurs iff $\hat{\boldsymbol{\rho}}_t - \cos(\theta)\mathbf{v}_0 = 0$, which is true only for $\theta = 0$, which indicates the identical solution as the former hence we have the unique representation

$$\hat{\boldsymbol{\rho}}_t = \cos(\theta) \mathbf{v}_0 + \sin(\theta) \mathbf{v}_0^{\perp}. \tag{91}$$

Using the same representation, it is straightforward to see that the unit length element $\hat{\boldsymbol{\rho}}_t^{\perp} = -\sin(\theta)\mathbf{v}_0 + \cos(\theta)\mathbf{v}_0^{\perp}$ satisfies

$$\langle \hat{\boldsymbol{\rho}}_t^{\perp}, \hat{\boldsymbol{\rho}}_t, \rangle = \langle -\sin(\theta)\mathbf{v}_0 + \cos(\theta)\mathbf{v}_0^{\perp}, \cos(\theta)\mathbf{v}_0 + \sin(\theta)\mathbf{v}_0^{\perp} \rangle = 0$$
(92)

and hence lies, in the plane whose normal is $\hat{\rho}_t$.

B.2 Proof of Lemma 4.3

Recalling the representation of the spectral estimate in the lifted problem we have

$$\hat{\mathbf{X}} = \mathcal{P}_S(\mathcal{F}^H \mathcal{F}(\boldsymbol{\rho}_t \boldsymbol{\rho}_t^H)) \tag{93}$$

where \mathcal{P}_S is the projection onto the set of symmetric matrices. $\hat{\mathbf{X}}_{PSD}$ is similarly written as

$$\hat{\mathbf{X}}_{PSD} = \mathcal{P}_{PSD}(\hat{\mathbf{X}}) = \mathcal{P}_{PSD}(\mathcal{F}^H \mathcal{F}(\boldsymbol{\rho}_t \boldsymbol{\rho}_t^H))$$
(94)

since the PSD-cone is a subset of the set of symmetric matrices S, and \mathcal{P}_{PSD} projection consists of projection onto S by \mathcal{P}_S , followed by suppression of negative eigenvalues. From Lemma 3.1, denoting $\tilde{\rho}_t = \rho_t \rho_t^H$ for the solution ρ_t obeying $\|\rho_t\| = 1$ we have

$$\|\hat{\mathbf{X}} - \tilde{\boldsymbol{\rho}}_{t}\| \leq \|\frac{1}{2}\mathcal{F}^{H}\mathcal{F}(\tilde{\boldsymbol{\rho}}_{t}) + \frac{1}{2}(\mathcal{F}^{H}\mathcal{F}(\tilde{\boldsymbol{\rho}}_{t}))^{H} - \tilde{\boldsymbol{\rho}}_{t}\|$$

$$\leq \frac{1}{2}\|\mathcal{F}^{H}\mathcal{F}(\tilde{\boldsymbol{\rho}}_{t}) - \tilde{\boldsymbol{\rho}}_{t}\| + \frac{1}{2}\|(\mathcal{F}^{H}\mathcal{F}(\tilde{\boldsymbol{\rho}}_{t}))^{H} - \tilde{\boldsymbol{\rho}}_{t}\|$$

$$\leq \frac{1}{2}\delta + \frac{1}{2}\|((\tilde{\boldsymbol{\rho}}_{t}) + \boldsymbol{\delta}(\tilde{\boldsymbol{\rho}}_{t}))^{H} - \tilde{\boldsymbol{\rho}}_{t}\|.$$

$$(95)$$

And since $\tilde{\rho}_t$ is Hermitian symmetric and that the spectral norm is unaffected by adjoint operation, we have

$$\frac{1}{2} \| ((\tilde{\rho}_t) + \delta(\tilde{\rho}_t))^H - \tilde{\rho}_t \| = \frac{1}{2} \| (\delta(\tilde{\rho}_t))^H \| = \frac{1}{2} \| \delta(\tilde{\rho}_t) \| \le \frac{1}{2} \delta.$$
 (97)

Hence the spectral norm of the lifted error is upper bounded as follows:

$$\|\hat{\mathbf{X}} - \tilde{\boldsymbol{\rho}}_t\| \le \delta. \tag{98}$$

For the maximal eigenvalue λ_0 of $\hat{\mathbf{X}}$, we can write

$$\lambda_0 \ge \boldsymbol{\rho}_t^H \hat{\mathbf{X}} \boldsymbol{\rho}_t = \boldsymbol{\rho}_t^H (\hat{\mathbf{X}} - \tilde{\boldsymbol{\rho}}_t) \boldsymbol{\rho}_t + 1 \ge 1 - \delta.$$
(99)

On the other hand, we have

$$|\mathbf{v}_0^H(\hat{\mathbf{X}} - \tilde{\boldsymbol{\rho}}_t)\mathbf{v}_0| \leq \|\hat{\mathbf{X}} - \tilde{\boldsymbol{\rho}}_t\| \leq \delta \rightarrow |\lambda_0 - |\mathbf{v}_0^H \boldsymbol{\rho}_t|^2| \leq \delta,$$

$$\lambda_0 \leq \delta + |\mathbf{v}_0^H \boldsymbol{\rho}_t|^2| \leq 1 + \delta.$$
(100)

Hence we obtain

$$1 - \delta \le \lambda_0 \le 1 + \delta. \tag{101}$$

Since the positive semi-definite estimate $\hat{\mathbf{X}}_{PSD}$ only differs from $\hat{\mathbf{X}}$ by the suppression of negative eigenvalues, and since spectral initialization only preserves the leading eigenvalue-eigenvector pair λ_0 , \mathbf{v}_0 and $\lambda_0 \geq 1 - \delta$ where $\delta > 0$, we have the identical $\boldsymbol{\rho}_0 = \sqrt{\lambda_0} \mathbf{v}_0$.

B.3 Proof of Lemma 4.4

We consider the case where the spectral estimate (33) is projected onto the positive semi-definite cone as in LRMR. In this case, the estimate obtained in spectral initialization is projected onto the

positive semi-definite cone to obtain $\hat{\mathbf{X}}_{PSD}$, which yields the identical initial point $\boldsymbol{\rho}_0$ per Lemma 4.3. Since its a symmetric, PSD matrix, we can decompose $\hat{\mathbf{X}}_{PSD}$ such that

$$\hat{\mathbf{X}}_{PSD} = \mathbf{S}_0 \mathbf{S}_0,$$

where \mathbf{S}_0 is a positive semi-definite matrix with its eigenvalues as $\sqrt{\lambda_{\hat{\mathbf{X}}_{PSD}}}$. Since

$$\mathbf{v}_0 := \underset{\|\mathbf{v}\|=1}{\operatorname{argmax}} \mathbf{v}^H \hat{\mathbf{X}}_{PSD} \mathbf{v}, \tag{102}$$

where $\mathbf{v}^H \hat{\mathbf{X}}_{PSD} \mathbf{v} = \mathbf{v}^H \mathbf{S}_0 \mathbf{S}_0 \mathbf{v} = ||\mathbf{S}_0 \mathbf{v}||^2$. Then using the definitions of $\hat{\boldsymbol{\rho}}_t$ and $\hat{\boldsymbol{\rho}}_t^{\perp}$ from Lemma 4.2, we have

$$\mathbf{S}_0 \hat{\boldsymbol{\rho}}_t = \cos(\theta) \mathbf{S}_0 \mathbf{v}_0 + \sin(\theta) \mathbf{S}_0 \mathbf{v}_0^{\perp}, \tag{103}$$

$$\mathbf{S}_0 \hat{\boldsymbol{\rho}}_t^{\perp} = -\sin(\theta) \mathbf{S}_0 \mathbf{v}_0 + \cos(\theta) \mathbf{S}_0, \mathbf{v}_0^{\perp}$$
(104)

and from Pythogorian theorem, since we have orthogonal components, we get

$$\|\mathbf{S}_{0}\hat{\boldsymbol{\rho}}_{t}\|^{2} = \cos^{2}(\theta)\|\mathbf{S}_{0}\mathbf{v}_{0}\|^{2} + \sin^{2}(\theta)\|\mathbf{S}_{0}\mathbf{v}_{0}^{\perp}\|^{2}, \tag{105}$$

$$\|\mathbf{S}_0 \hat{\boldsymbol{\rho}}_t^{\perp}\|^2 = \sin^2(\theta) \|\mathbf{S}_0 \mathbf{v}_0\|^2 + \cos^2(\theta) \|\mathbf{S}_0 \mathbf{v}_0^{\perp}\|^2. \tag{106}$$

Consider the expression $f = \sin^2(\theta) \|\mathbf{S}_0 \hat{\boldsymbol{\rho}}_t\|^2 - \|\mathbf{S}_0 \hat{\boldsymbol{\rho}}_t^{\perp}\|^2$. Following the algebra in [45], we have

$$f = \sin^{2}(\theta) \left(\cos^{2}(\theta) \|\mathbf{S}_{0}\mathbf{v}_{0}\|^{2} + \sin^{2}(\theta) \|\mathbf{S}_{0}\mathbf{v}_{0}^{\perp}\|^{2}\right) - \left(\sin^{2}(\theta) \|\mathbf{S}_{0}\mathbf{v}_{0}\|^{2} + \cos^{2}(\theta) \|\mathbf{S}_{0}\mathbf{v}_{0}^{\perp}\|^{2}\right)$$

$$= \sin^{2}(\theta) \left(\cos^{2}(\theta) \|\mathbf{S}_{0}\mathbf{v}_{0}\|^{2} - \|\mathbf{S}_{0}\mathbf{v}_{0}\|^{2} + \sin^{2}(\theta) \|\mathbf{S}_{0}\mathbf{v}_{0}^{\perp}\|^{2}\right) - \cos^{2}(\theta) \|\mathbf{S}_{0}\mathbf{v}_{0}^{\perp}\|^{2},$$

which finally yields

$$f = \sin^4(\theta) \left(\|\mathbf{S}_0 \mathbf{v}_0^{\perp}\|^2 - \|\mathbf{S}_0 \mathbf{v}_0\|^2 \right) - \cos^2(\theta) \|\mathbf{S}_0 \mathbf{v}_0^{\perp}\|^2.$$
 (107)

Since \mathbf{v}_0 is the unit vector that maximizes $\|\mathbf{S}_0\mathbf{v}\|^2$, with the fact that \mathbf{v}_0^{\perp} is also a unit vector, this expression is always non-positive, hence

$$\sin^{2}(\theta) \|\mathbf{S}_{0}\hat{\boldsymbol{\rho}}_{t}\|^{2} - \|\mathbf{S}_{0}\hat{\boldsymbol{\rho}}_{t}^{\perp}\|^{2} \leq 0,$$

$$\sin^{2}(\theta) \leq \frac{\|\mathbf{S}_{0}\hat{\boldsymbol{\rho}}_{t}^{\perp}\|^{2}}{\|\mathbf{S}_{0}\hat{\boldsymbol{\rho}}_{t}\|^{2}}.$$
(108)

Equivalently, expressing the upper bound with the spectral estimate, we obtain

$$\sin^2(\theta) \le \frac{(\hat{\boldsymbol{\rho}}_t^{\perp})^H \hat{\mathbf{X}}_{PSD} \hat{\boldsymbol{\rho}}_t^{\perp}}{\hat{\boldsymbol{\rho}}_t^H \hat{\mathbf{X}}_{PSD} \hat{\boldsymbol{\rho}}_t}.$$
(109)

Now we consider the spectral estimate $\hat{\mathbf{X}}_{PSD}$. We know that $\hat{\mathbf{X}}_{PSD}$ is obtained by projecting the intermediate estimate $\mathbf{Y} = \mathcal{F}^H \mathcal{F}(\tilde{\boldsymbol{\rho}}_t)$ onto the feasible set of PSD matrices as defined in Lemma 4.3. From Lemma 3.1 for the RIP-1 property of \mathcal{F} , we know that $\mathcal{F}^H \mathcal{F}$ is almost an identity on

the domain of rank-1, PSD matrices, hence we can write the perturbation model

$$\hat{\mathbf{X}}_{PSD} = \mathcal{P}_{PSD} \left(\tilde{\boldsymbol{\rho}}_t + \boldsymbol{\delta}[\tilde{\boldsymbol{\rho}}_t] \right) \tag{110}$$

Since PSD matrices is a convex set and a projection operator of a convex set is non-expansive, we have the following

$$\|\hat{\mathbf{X}}_{PSD} - \tilde{\boldsymbol{\rho}}_t\|_F \le \|\mathbf{Y} - \tilde{\boldsymbol{\rho}}_t\|_F. \tag{111}$$

Setting $\hat{\mathbf{X}}_{PSD} = \tilde{\boldsymbol{\rho}}_t + \tilde{\mathbf{e}}$, the upper bound in (109) can be written as

$$\sin^2(\theta) \le \frac{(\hat{\boldsymbol{\rho}}_t^{\perp})^H \tilde{\boldsymbol{\rho}}_t \hat{\boldsymbol{\rho}}_t^{\perp} + (\hat{\boldsymbol{\rho}}_t^{\perp})^H \tilde{\mathbf{e}} \hat{\boldsymbol{\rho}}_t^{\perp}}{\hat{\boldsymbol{\rho}}_t^H \tilde{\boldsymbol{\rho}}_t \hat{\boldsymbol{\rho}}_t + \hat{\boldsymbol{\rho}}_t^H \tilde{\mathbf{e}} \hat{\boldsymbol{\rho}}_t^{\perp}}.$$
(112)

Since we have that $\tilde{\rho}_t = \rho_t \rho_t^H$, the bound reduces to

$$\sin^2(\theta) \le \frac{(\hat{\boldsymbol{\rho}}_t^{\perp})^H \tilde{\mathbf{e}} \hat{\boldsymbol{\rho}}_t^{\perp}}{1 + \hat{\boldsymbol{\rho}}_t^H \tilde{\mathbf{e}} \hat{\boldsymbol{\rho}}_t}$$
(113)

as $\hat{\boldsymbol{\rho}}_t^{\perp}$ is orthogonal to $\hat{\boldsymbol{\rho}}_t$ and the global phase component in $\hat{\boldsymbol{\rho}}_t = e^{j\Phi(v_0)}\boldsymbol{\rho}_t$ vanishes in the quadratic form. Moreover, we know that $(\hat{\boldsymbol{\rho}}_t^{\perp})^H \tilde{\mathbf{e}} \hat{\boldsymbol{\rho}}_t^{\perp}$ is non-negative from positive semi-definitivity of $\hat{\mathbf{X}}_{PSD}$. Hence we further upper bound the numerator by the spectral norm of $\tilde{\mathbf{e}}$, and follow with the series of bounds

$$\sin^{2}(\theta) \leq \frac{\|\tilde{\mathbf{e}}\|_{2}}{1 + \hat{\boldsymbol{\rho}}_{t}^{H}\tilde{\mathbf{e}}\hat{\boldsymbol{\rho}}_{t}} \leq \frac{\|\tilde{\mathbf{e}}\|_{F}}{1 + \hat{\boldsymbol{\rho}}_{t}^{H}\tilde{\mathbf{e}}\hat{\boldsymbol{\rho}}_{t}} \leq \frac{\|\boldsymbol{\delta}(\tilde{\boldsymbol{\rho}}_{t})\|_{F}}{1 + \hat{\boldsymbol{\rho}}_{t}^{H}\tilde{\mathbf{e}}\hat{\boldsymbol{\rho}}_{t}} \leq \frac{\|\boldsymbol{\delta}\|\|\tilde{\boldsymbol{\rho}}_{t}\|_{F}}{1 + \hat{\boldsymbol{\rho}}_{t}^{H}\tilde{\mathbf{e}}\hat{\boldsymbol{\rho}}_{t}} \leq \frac{\delta}{1 + \hat{\boldsymbol{\rho}}_{t}^{H}\tilde{\mathbf{e}}\hat{\boldsymbol{\rho}}_{t}}$$
(114)

where the last two inequalities follow from the non-expansiveness property of the projection operator onto the convex PSD cone, the Cauchy-Scwartz inequality, and the definition of δ from Lemma 3.1, such that the spectral norm of δ is upper bounded by the RIC- δ of \mathcal{F} . For the term in the denominator, since we established that $\|\tilde{\mathbf{e}}\|_2 \leq \delta$, we have that $-\delta \leq \hat{\boldsymbol{\rho}}_t^H \tilde{\mathbf{e}} \hat{\boldsymbol{\rho}}_t \leq \delta$ to finally obtain

$$\sin^2(\theta) \le \frac{\delta}{1 + \hat{\rho}_t^H \tilde{\mathbf{e}} \hat{\rho}_t} \le \frac{\delta}{1 - \delta}.$$
 (115)

B.4 Proof of Lemma 4.5

B.4.1 The Upper Bound

Noting that $\hat{\rho}_t$ is the closest solution in P to an estimate ρ , we define $\rho_e = \rho - \hat{\rho}_t$. Since $\rho \in E(\epsilon)$, $\operatorname{dist}(\rho, \rho_t) = ||\rho_e|| \le \epsilon$, and from reverse triangle inequality we have

$$|\|\boldsymbol{\rho}\| - \|\hat{\boldsymbol{\rho}}_t\|| \le \|\boldsymbol{\rho} - \hat{\boldsymbol{\rho}}_t\| \le \epsilon$$

Since $\|\hat{\rho}_t\| = \|\rho_t\| = 1$, we have that $1 - \epsilon \le \|\rho\| \le 1 + \epsilon$. Having $\hat{\rho}_t \hat{\rho}_t^H = \rho_t \rho_t^H$, we let $\tilde{\mathbf{e}} = \rho \rho^H - \hat{\rho}_t \hat{\rho}_t^H$ denote the error in the lifted problem. Then, writing the lifted error $\tilde{\rho}_e = \rho_e \rho_e^H$

as

$$\rho_e \rho_e^H = (\rho - \hat{\rho}_t)(\rho - \hat{\rho}_t)^H = \rho \rho^H - \rho \hat{\rho}_t^H - \hat{\rho}_t \rho^H + \hat{\rho}_t \hat{\rho}_t^H + (2\hat{\rho}_t \hat{\rho}_t^H - 2\hat{\rho}_t \hat{\rho}_t^H)$$

$$= \tilde{\mathbf{e}} - (\rho - \hat{\rho}_t)\hat{\rho}_t^H - \hat{\rho}_t(\rho^H - \hat{\rho}_t^H), \tag{116}$$

finally yields the expression

$$\tilde{\mathbf{e}} = \boldsymbol{\rho}_e \boldsymbol{\rho}_e^H + \boldsymbol{\rho}_e \hat{\boldsymbol{\rho}}_t^H + \hat{\boldsymbol{\rho}}_t \boldsymbol{\rho}_e^H \tag{117}$$

for the error in the lifted domain. We can then write the upper bound for $\|\tilde{\mathbf{e}}\|_F$ as

$$\|\tilde{\mathbf{e}}\|_{F} \leq \|\boldsymbol{\rho}_{e}\boldsymbol{\rho}_{e}^{H}\|_{F} + \|\boldsymbol{\rho}_{e}\hat{\boldsymbol{\rho}}_{t}^{H}\|_{F} + \|\hat{\boldsymbol{\rho}}_{t}\boldsymbol{\rho}_{e}^{H}\|_{F}. \tag{118}$$

Since all the arguments of the Frobenius norm in the right-hand-side have rank-1, we have $\|\cdot\|_2 = \|\cdot\|_F$. Knowing that $\|\boldsymbol{\rho}_t\| = 1$ we get

$$\|\tilde{\mathbf{e}}\|_F \le 2\|\hat{\boldsymbol{\rho}}_t\|\|\boldsymbol{\rho}_e\| + \|\boldsymbol{\rho}_e\|^2 \le (2+\epsilon)\|\boldsymbol{\rho}_e\|.$$
 (119)

Hence we obtain the upper bound

$$\|\boldsymbol{\rho}\boldsymbol{\rho}^H - \boldsymbol{\rho}_t\boldsymbol{\rho}_t^H\|_F \le (2 + \epsilon)\operatorname{dist}(\boldsymbol{\rho}, \boldsymbol{\rho}_t).$$
 (120)

B.4.2 The Lower Bound

Expanding the error in the lifted domain, we get

$$\|\tilde{\mathbf{e}}\|_F^2 = \|\boldsymbol{\rho}\boldsymbol{\rho}^H\|_F^2 + \|\boldsymbol{\rho}_t\boldsymbol{\rho}_t^H\|_F^2 - 2\operatorname{Re}\langle\boldsymbol{\rho}\boldsymbol{\rho}^H,\boldsymbol{\rho}_t\boldsymbol{\rho}_t^H\rangle_F. \tag{121}$$

Since we have the rank-1 lifted signals, the Frobenius norms and the inner product reduce to

$$\|\tilde{\mathbf{e}}\|_{F}^{2} = \|\boldsymbol{\rho}\|^{4} + \|\boldsymbol{\rho}_{t}\|^{4} - 2|\langle \boldsymbol{\rho}, \boldsymbol{\rho}_{t} \rangle|^{2} = (\|\boldsymbol{\rho}\|^{4} - |\langle \boldsymbol{\rho}, \boldsymbol{\rho}_{t} \rangle|^{2}) + (\|\boldsymbol{\rho}_{t}\|^{4} - |\langle \boldsymbol{\rho}, \boldsymbol{\rho}_{t} \rangle|^{2})$$

$$= (\|\boldsymbol{\rho}\|^{2} + |\langle \boldsymbol{\rho}, \boldsymbol{\rho}_{t} \rangle|)(\|\boldsymbol{\rho}\|^{2} - |\langle \boldsymbol{\rho}, \boldsymbol{\rho}_{t} \rangle|) + (\|\boldsymbol{\rho}_{t}\|^{2} + |\langle \boldsymbol{\rho}, \boldsymbol{\rho}_{t} \rangle|)(\|\boldsymbol{\rho}_{t}\|^{2} - |\langle \boldsymbol{\rho}, \boldsymbol{\rho}_{t} \rangle|). \quad (122)$$

Having dist² $(\boldsymbol{\rho}, \boldsymbol{\rho}_t) = \|\boldsymbol{\rho}\|^2 + \|\boldsymbol{\rho}_t\|^2 - 2|\langle \boldsymbol{\rho}, \boldsymbol{\rho}_t \rangle| = \|\boldsymbol{\rho} - \hat{\boldsymbol{\rho}}_t\| \ge 0$, we can lower bound (121) using (122) as

$$\|\tilde{\mathbf{e}}\|_F^2 \ge \min\left((\|\boldsymbol{\rho}\|^2 + |\langle \boldsymbol{\rho}, \boldsymbol{\rho}_t \rangle|), (\|\boldsymbol{\rho}_t\|^2 + |\langle \boldsymbol{\rho}, \boldsymbol{\rho}_t \rangle|)\right) (\|\boldsymbol{\rho}\|^2 + \|\boldsymbol{\rho}_t\|^2 - 2|\langle \boldsymbol{\rho}, \boldsymbol{\rho}_t \rangle|). \tag{123}$$

Knowing that $\operatorname{dist}^2(\boldsymbol{\rho}, \boldsymbol{\rho}_t) \leq \epsilon^2$ and the result from the reverse triangle inequality on $\|\boldsymbol{\rho}\|$, the terms within the minimization are further lower bounded using

$$2|\langle \boldsymbol{\rho}, \boldsymbol{\rho}_t \rangle| \geq \|\boldsymbol{\rho}\|^2 + \|\boldsymbol{\rho}_t\|^2 - \epsilon^2$$
$$|\langle \boldsymbol{\rho}, \boldsymbol{\rho}_t \rangle| \geq (1 - \epsilon). \tag{124}$$

We then get the bound on the scalar multiplying dist²(ρ, ρ_t) as

$$\min\left(\left(\|\boldsymbol{\rho}\|^2 + |\langle \boldsymbol{\rho}, \boldsymbol{\rho}_t \rangle|\right), \left(\|\boldsymbol{\rho}_t\|^2 + |\langle \boldsymbol{\rho}, \boldsymbol{\rho}_t \rangle|\right)\right) \ge (1 - \epsilon)^2 + (1 - \epsilon),\tag{125}$$

which yields the final lower bound as

$$\|\boldsymbol{\rho}\boldsymbol{\rho}^H - \boldsymbol{\rho}_t \boldsymbol{\rho}_t^H\|_F \ge \sqrt{(1-\epsilon)(2-\epsilon)} \operatorname{dist}(\boldsymbol{\rho}, \boldsymbol{\rho}_t).$$
 (126)

B.5 Proof of Lemma 4.6

From the adjoint property of the inner product we have

$$\|\mathcal{F}(\boldsymbol{\rho}\boldsymbol{\rho}^H - \boldsymbol{\rho}_t\boldsymbol{\rho}_t^H)\|^2 = \langle \boldsymbol{\rho}\boldsymbol{\rho}^H - \boldsymbol{\rho}_t\boldsymbol{\rho}_t^H, \mathcal{F}^H\mathcal{F}(\boldsymbol{\rho}\boldsymbol{\rho}^H - \boldsymbol{\rho}_t\boldsymbol{\rho}_t^H)\rangle_F.$$

Splitting the linear operator $\mathcal{F}^H\mathcal{F}$ over the rank-1 inputs, we can use the perturbation model from Lemma 3.1 such that

$$= \langle \boldsymbol{\rho} \boldsymbol{\rho}^{H} - \boldsymbol{\rho}_{t} \boldsymbol{\rho}_{t}^{H}, \mathcal{F}^{H} \mathcal{F}(\boldsymbol{\rho} \boldsymbol{\rho}^{H}) \rangle_{F} - \langle \boldsymbol{\rho} \boldsymbol{\rho}^{H} - \boldsymbol{\rho}_{t} \boldsymbol{\rho}_{t}^{H}, \mathcal{F}^{H} \mathcal{F}(\boldsymbol{\rho}_{t} \boldsymbol{\rho}_{t}^{H}) \rangle_{F}$$

$$= \| \boldsymbol{\rho} \boldsymbol{\rho}^{H} - \boldsymbol{\rho}_{t} \boldsymbol{\rho}_{t}^{H} \|_{F}^{2} + \langle \boldsymbol{\rho} \boldsymbol{\rho}^{H} - \boldsymbol{\rho}_{t} \boldsymbol{\rho}_{t}^{H}, \boldsymbol{\delta}(\boldsymbol{\rho} \boldsymbol{\rho}^{H}) - \boldsymbol{\delta}(\boldsymbol{\rho}_{t} \boldsymbol{\rho}_{t}^{H}) \rangle_{F}. \tag{127}$$

Using the representation of $\tilde{\mathbf{e}} = \boldsymbol{\rho} \boldsymbol{\rho}^H - \boldsymbol{\rho}_t \boldsymbol{\rho}_t^H$ in (117), and extending the domain of $\boldsymbol{\delta}$ on the set of rank-1 matrices, from the linearity of $\boldsymbol{\delta}$ we have

$$\delta(\rho \rho^H) = \delta(\rho_e \rho_e^H) + \delta(\rho_e \hat{\rho}_t^H) + \delta(\hat{\rho}_t \rho_e^H) + \delta(\rho_t \rho_e^H). \tag{128}$$

Plugging (128) into (127), and applying Cauchy-Schwartz and triangle inequalities on absolute value of the Frobenius inner product term, we have

$$|\langle \boldsymbol{\rho} \boldsymbol{\rho}^{H} - \boldsymbol{\rho}_{t} \boldsymbol{\rho}_{t}^{H}, \boldsymbol{\delta}(\boldsymbol{\rho}_{e} \boldsymbol{\rho}_{e}^{H}) + \boldsymbol{\delta}(\boldsymbol{\rho}_{e} \hat{\boldsymbol{\rho}}_{t}^{H}) + \boldsymbol{\delta}(\hat{\boldsymbol{\rho}}_{t} \boldsymbol{\rho}_{e}^{H}) \rangle_{F}| \leq \cdots$$

$$\cdots \|\boldsymbol{\rho} \boldsymbol{\rho}^{H} - \boldsymbol{\rho}_{t} \boldsymbol{\rho}_{t}^{H}\|_{F} \left(\|\boldsymbol{\delta}(\boldsymbol{\rho}_{e} \boldsymbol{\rho}_{e}^{H})\|_{F} + \|\boldsymbol{\delta}(\boldsymbol{\rho}_{e} \hat{\boldsymbol{\rho}}_{t}^{H})\|_{F} + \|\boldsymbol{\delta}(\hat{\boldsymbol{\rho}}_{t} \boldsymbol{\rho}_{e}^{H})\|_{F} \right).$$

$$(129)$$

Furthermore, from Lemma 3.1, for a RIP-1 property of \mathcal{F} with RIC- δ_1 , for (129) we have

$$\leq \|\rho \rho^{H} - \rho_{t} \rho_{t}^{H} \|_{F} \|\delta\| \left(\|\rho_{e} \rho_{e}^{H} \|_{F} + \|\rho_{e} \hat{\rho}_{t}^{H} \|_{F} + \|\hat{\rho}_{t} \rho_{e}^{H} \|_{F} \right)
\leq \delta_{1} \|\rho \rho^{H} - \rho_{t} \rho_{t}^{H} \|_{F} \left(\|\rho_{e} \rho_{e}^{H} \|_{F} + \|\rho_{e} \hat{\rho}_{t}^{H} \|_{F} + \|\hat{\rho}_{t} \rho_{e}^{H} \|_{F} \right).$$
(130)

Invoking the rank-1 property on the terms inside the parenthesis in (130), the Frobenius norms can be computed by the spectral norm of the arguments, i.e., $\|\cdot\| = \|\cdot\|_F$ for a rank-1 argument. Then, having $\|\boldsymbol{\rho}_t\| = 1$, for the right-hand-side we obtain

$$|\langle \boldsymbol{\rho} \boldsymbol{\rho}^{H} - \boldsymbol{\rho}_{t} \boldsymbol{\rho}_{t}^{H}, \boldsymbol{\delta}(\boldsymbol{\rho} \boldsymbol{\rho}^{H}) - \boldsymbol{\delta}(\boldsymbol{\rho}_{t} \boldsymbol{\rho}_{t}^{H}) \rangle_{F}| \leq \delta_{1} \|\boldsymbol{\rho} \boldsymbol{\rho}^{H} - \boldsymbol{\rho}_{t} \boldsymbol{\rho}_{t}^{H} \|_{F} \left(2 \|\boldsymbol{\rho}_{t}\| \|\boldsymbol{\rho}_{e}\| + \|\boldsymbol{\rho}_{e}\|^{2} \right) \\ \leq \delta_{1} (2 + \epsilon) \|\boldsymbol{\rho} \boldsymbol{\rho}^{H} - \boldsymbol{\rho}_{t} \boldsymbol{\rho}_{t}^{H} \|_{F} \operatorname{dist}(\boldsymbol{\rho}, \boldsymbol{\rho}_{t}).$$
(131)

Using the bound

$$\sqrt{(1-\epsilon)(2-\epsilon)}\operatorname{dist}(\boldsymbol{\rho},\boldsymbol{\rho}_t) \leq \|\boldsymbol{\rho}\boldsymbol{\rho}^H - \boldsymbol{\rho}_t\boldsymbol{\rho}_t^H\|_F, \tag{132}$$

from Lemma 4.5, we finally obtain the upper bound on the perturbation on $\|\boldsymbol{\rho}\boldsymbol{\rho}^H - \boldsymbol{\rho}_t\boldsymbol{\rho}_t^H\|_F^2$ as

$$|\langle \boldsymbol{\rho} \boldsymbol{\rho}^H - \boldsymbol{\rho}_t \boldsymbol{\rho}_t^H, \boldsymbol{\delta}(\boldsymbol{\rho} \boldsymbol{\rho}^H) - \boldsymbol{\delta}(\boldsymbol{\rho}_t \boldsymbol{\rho}_t^H) \rangle_F| \le \delta_1 \frac{2 + \epsilon}{\sqrt{(1 - \epsilon)(2 - \epsilon)}} \|\boldsymbol{\rho} \boldsymbol{\rho}^H - \boldsymbol{\rho}_t \boldsymbol{\rho}_t^H\|_F^2.$$
(133)

Hence, setting $\delta_2 = \delta_1 \frac{2+\epsilon}{\sqrt{(1-\epsilon)(2-\epsilon)}}$, we have the local RIP-2 condition satisfied with RIC- δ_2 .

B.6 Proof of Lemma 4.7

Having $\tilde{\rho}_t = \rho_t \rho_t^H = \hat{\rho}_t \hat{\rho}_t^H$, we re-write the gradient term in (58) as

$$\nabla \mathcal{J}(\boldsymbol{\rho}) = \|\boldsymbol{\rho}\|^2 \boldsymbol{\rho} - (\hat{\boldsymbol{\rho}}_t^H \boldsymbol{\rho}) \hat{\boldsymbol{\rho}}_t + \mathcal{P}_S(\boldsymbol{\delta}(\tilde{\mathbf{e}})) \boldsymbol{\rho}$$

where $\tilde{\mathbf{e}} = \boldsymbol{\rho} \boldsymbol{\rho}^H - \boldsymbol{\rho}_t \boldsymbol{\rho}_t^H$. Then, simply from the triangle inequality and the definition of projection operator on the set of symmetric matrices, we get

$$\|\nabla \mathcal{J}(\boldsymbol{\rho})\| \leq \|\|\boldsymbol{\rho}\|^{2} \boldsymbol{\rho} - (\hat{\boldsymbol{\rho}}_{t}^{H} \boldsymbol{\rho}) \hat{\boldsymbol{\rho}}_{t} \| + \frac{1}{2} \|\boldsymbol{\delta}(\tilde{\mathbf{e}})\|_{2} \|\boldsymbol{\rho}\| + \frac{1}{2} \|\boldsymbol{\delta}(\tilde{\mathbf{e}})^{H}\|_{2} \|\boldsymbol{\rho}\| \leq \|\|\boldsymbol{\rho}\|^{2} \boldsymbol{\rho} - (\hat{\boldsymbol{\rho}}_{t}^{H} \boldsymbol{\rho}) \hat{\boldsymbol{\rho}}_{t} \| + \|\boldsymbol{\delta}(\tilde{\mathbf{e}})\|_{2} \|\boldsymbol{\rho}\|,$$
(134)

since the spectral norm is unchanged by Hermitian transpose operation. Invoking Lemma 4.6, we further upper bound the second term in the right-hand-side using the RIC- δ_2 , followed by upper bounding the first term.

$$\|\nabla \mathcal{J}(\boldsymbol{\rho})\| \le \|\|\boldsymbol{\rho}\|^2 \boldsymbol{\rho} - (\hat{\boldsymbol{\rho}}_t^H \boldsymbol{\rho}) \hat{\boldsymbol{\rho}}_t \| + \delta_2 \|\tilde{\mathbf{e}}\|_F \|\boldsymbol{\rho}\| \le \|\boldsymbol{\rho}\| \left((\|\boldsymbol{\rho}\| + \|\boldsymbol{\rho}_t\|) \|\boldsymbol{\rho} - \hat{\boldsymbol{\rho}}_t\| + \delta_2 \|\tilde{\mathbf{e}}\|_F \right). \tag{135}$$

Using the fact that $\rho \in E(\epsilon)$, and $\hat{\rho}_t = e^{i\phi(\rho)}\rho_t$, we know that $1 - \epsilon \leq ||\rho|| \leq 1 + \epsilon$ from triangle and reverse triangle inequalities. Furthermore, from Lemma 4.5, we have $||\tilde{\mathbf{e}}||_F \leq (2 + \epsilon)||\rho - \hat{\rho}_t||$. Hence,

$$\|\nabla \mathcal{J}(\boldsymbol{\rho})\| \le (1+\epsilon) ((2+\epsilon)\|\boldsymbol{\rho} - \hat{\boldsymbol{\rho}}_t\| + \delta_2(2+\epsilon)\|\boldsymbol{\rho} - \hat{\boldsymbol{\rho}}_t\|) \le (1+\epsilon)(1+\delta_2)(2+\epsilon)\|\boldsymbol{\rho} - \hat{\boldsymbol{\rho}}_t\|.$$
 (136)

Thereby, setting $c = (1 + \epsilon)(1 + \delta_2)(2 + \epsilon)$ the right-hand-side of the regularity condition is upper bounded as

$$\frac{1}{\alpha} \|\boldsymbol{\rho} - \hat{\boldsymbol{\rho}}_t\|^2 + \frac{1}{\beta} \|\nabla \mathcal{J}(\boldsymbol{\rho})\|^2 \le \left(\frac{1}{\alpha} + \frac{c^2}{\beta}\right) \|\boldsymbol{\rho} - \hat{\boldsymbol{\rho}}_t\|^2$$
(137)

and the regularity condition (60) is established if the following condition holds:

$$\operatorname{Re}\left(\langle \nabla \mathcal{J}(\boldsymbol{\rho}), (\boldsymbol{\rho} - e^{\mathrm{i}\phi(\boldsymbol{\rho})}\boldsymbol{\rho}_t)\rangle\right) \ge \left(\frac{1}{\alpha} + \frac{c^2}{\beta}\right) \operatorname{dist}^2(\boldsymbol{\rho}, \boldsymbol{\rho}_t). \tag{138}$$

B.7 Proof of Lemma 4.8

Indeed, the form that the regularity condition is nothing but the restricted strong convexity condition. Since $\nabla \mathcal{J}(\boldsymbol{\rho}_t e^{i\Phi(\boldsymbol{\rho})}) = 0$ for any $\Phi(\boldsymbol{\rho}) = \Phi_0 \in [0, 2\pi)$, by definition, one can equivalently write (64) as

$$\operatorname{Re}\left(\langle \left(\nabla \mathcal{J}(\boldsymbol{\rho}) - \nabla \mathcal{J}(\boldsymbol{\rho}_t e^{i\Phi(\boldsymbol{\rho})})\right), (\boldsymbol{\rho} - \boldsymbol{\rho}_t e^{i\phi(\boldsymbol{\rho})})\rangle\right) \ge \eta \|\boldsymbol{\rho} - \boldsymbol{\rho}_t e^{i\phi(\boldsymbol{\rho})}\|^2, \tag{139}$$

where $\eta = (\frac{1}{\alpha} + \frac{c^2}{\beta})$. Reorganizing the terms, we have

$$\operatorname{Re}\left(\langle\left(\nabla \mathcal{J}(\boldsymbol{\rho}) - \nabla \mathcal{J}(\boldsymbol{\rho}_t e^{i\Phi(\boldsymbol{\rho})})\right) - \eta(\boldsymbol{\rho} - \boldsymbol{\rho}_t e^{i\phi(\boldsymbol{\rho})}), (\boldsymbol{\rho} - \boldsymbol{\rho}_t e^{i\phi(\boldsymbol{\rho})})\rangle\right) \ge 0. \tag{140}$$

Letting $g(\boldsymbol{\rho}) = \mathcal{J}(\boldsymbol{\rho}) - \frac{\eta}{2} \|\boldsymbol{\rho}\|^2$, we can write (140) as:

Re
$$\left(\left\langle \left(\nabla g(\boldsymbol{\rho}) - \nabla g(\boldsymbol{\rho}_t e^{i\Phi(\boldsymbol{\rho})}\right)\right), (\boldsymbol{\rho} - \boldsymbol{\rho}_t e^{i\phi(\boldsymbol{\rho})})\right\rangle \right) \ge 0.$$
 (141)

For any ρ in the ϵ -ball of $\rho_t e^{i\Phi(\rho)}$, (141) is merely the local convexity condition for g at point $\hat{\rho}_t = \rho_t e^{i\Phi(\rho)}$. Since the ϵ -ball around $\hat{\rho}_t$ is a convex set, we can use the equivalent condition

$$g(\boldsymbol{\rho}) \ge g(\boldsymbol{\rho}_t e^{i\Phi(\boldsymbol{\rho})}) + \operatorname{Re}\left(\nabla g(\boldsymbol{\rho}_t e^{i\Phi(\boldsymbol{\rho})})^H (\boldsymbol{\rho} - \boldsymbol{\rho}_t e^{i\Phi(\boldsymbol{\rho})})\right).$$
 (142)

Plugging in the definition for g, we obtain

$$\mathcal{J}(\boldsymbol{\rho}) \ge \mathcal{J}(\boldsymbol{\rho}_t e^{i\Phi(\boldsymbol{\rho})}) + \operatorname{Re}\left(\nabla \mathcal{J}(\boldsymbol{\rho}_t e^{i\Phi(\boldsymbol{\rho})})^H (\boldsymbol{\rho} - \boldsymbol{\rho}_t e^{i\Phi(\boldsymbol{\rho})})\right) + \frac{\eta}{2} \|\boldsymbol{\rho} - \boldsymbol{\rho}_t e^{i\Phi(\boldsymbol{\rho})}\|^2. \tag{143}$$

Since $\rho_t e^{i\Phi(\rho)}$ is a global minimizer of \mathcal{J} , it satisfies the first order optimality condition with $\nabla \mathcal{J}(\rho_t e^{i\Phi(\rho)}) = 0$, and the minimum it attains is 0. Hence the condition reduces to

$$\mathcal{J}(\boldsymbol{\rho}) \ge \frac{\eta}{2} \operatorname{dist}^2(\boldsymbol{\rho}, \boldsymbol{\rho}_t). \tag{144}$$

C Lemmas for Theorem 3.2

C.1 Proof of Lemma 4.9

For the intermediate stage, Y, of the spectral estimate, we write

$$\mathbf{Y} = \mathcal{F}^H \mathcal{F}(\boldsymbol{\rho}_t \boldsymbol{\rho}_t) = \frac{1}{M} \sum_{m=1}^{M} ((\mathbf{L}_i^m)^H \boldsymbol{\rho}_t \boldsymbol{\rho}_t^H \mathbf{L}_j^m) \mathbf{L}_i^m (\mathbf{L}_j^m)^H.$$
(145)

Reorganizing the terms in (145) and taking the expectation, we have

$$\mathbb{E}[\mathbf{Y}] = \frac{1}{M} \sum_{m=1}^{M} \mathbb{E}[(\mathbf{L}_{i}^{m}(\mathbf{L}_{i}^{m})^{H} \boldsymbol{\rho}_{t})(\mathbf{L}_{j}^{m}(\mathbf{L}_{j}^{m})^{H} \boldsymbol{\rho}_{t})^{H}].$$
(146)

For fixed m, and having ρ_t is independent of sampling vectors, the $N \times N$ matrix inside the summation has the entries of the form,

$$\sum_{n=1}^{N} \sum_{n'=1}^{N} \mathbb{E}[(\mathbf{L}_{i}^{m})_{k}(\overline{\mathbf{L}_{i}^{m}})_{n}(\overline{\mathbf{L}_{j}^{m}})_{l}(\mathbf{L}_{j}^{m})_{n'}]\boldsymbol{\rho}_{tn}\overline{\boldsymbol{\rho}_{t}}_{n'}, \tag{147}$$

where k,l denote the row and column indexes, respectfully. Since \mathbf{L}_i^m and \mathbf{L}_j^m are independent of each other and have i.i.d. entries, the 4^{th} moments of Gaussian entries are removed as $\mathbb{E}[(\mathbf{L}_i^m)_k(\overline{\mathbf{L}_i^m})_n(\overline{\mathbf{L}_j^m})_l(\mathbf{L}_j^m)_{n'}] = \mathbb{E}[(\mathbf{L}_i^m)_k(\overline{\mathbf{L}_i^m})_n]\mathbb{E}[(\overline{\mathbf{L}_j^m})_l(\mathbf{L}_j^m)_{n'}]$, in which the expectations are only non-zero for n=k, n'=l, yielding

$$= \mathbb{E}[|(\mathbf{L}_i^m)_k|^2]\mathbb{E}[|(\mathbf{L}_j^m)_l|^2]\boldsymbol{\rho}_{tk}\overline{\boldsymbol{\rho}_{tl}}, \tag{148}$$

where $\mathbf{L}_i^m, \mathbf{L}_i^m \sim \mathcal{N}(0, \frac{1}{2}\mathbf{I}) + i\mathcal{N}(0, \frac{1}{2}\mathbf{I})$ have unit variance. Hence,

$$\mathbb{E}[\mathbf{Y}]_{k,l} = \boldsymbol{\rho}_{tk} \overline{\boldsymbol{\rho}_{tl}},\tag{149}$$

which is precisely equal to $\mathbb{E}[\mathbf{Y}] = \boldsymbol{\rho}_t \boldsymbol{\rho}_t^H$.

C.2 Proof of Lemma 4.10

We use the machinery in the proof of the concentration bound of the Hessian in [1].⁶ By unitary invariance, we take $\rho_t = \mathbf{e}_1$, where \mathbf{e}_1 is the first standard basis vector. We want to establish that

$$\|\frac{1}{M}\sum_{m=1}^{M}\overline{(\mathbf{L}_{i}^{m})_{1}}(\mathbf{L}_{j}^{m})_{1}\mathbf{L}_{i}^{m}(\mathbf{L}_{j}^{m})^{H} - \mathbf{e}_{1}\mathbf{e}_{1}^{T}\| \leq \delta.$$

$$(150)$$

The inequality in (150) is equivalent to

$$I_0(\mathbf{y}) := \left| \mathbf{y}^H \left(\frac{1}{M} \sum_{m=1}^M \overline{(\mathbf{L}_i^m)_1} (\mathbf{L}_j^m)_1 \mathbf{L}_i^m (\mathbf{L}_j^m)^H - \mathbf{e}_1 \mathbf{e}_1^T \right) \mathbf{y} \right|$$
 (151)

$$= \left| \frac{1}{M} \sum_{m=1}^{M} \overline{(\mathbf{L}_{i}^{m})_{1}} (\mathbf{L}_{j}^{m})_{1} (\mathbf{y}^{H} \mathbf{L}_{i}^{m} (\mathbf{L}_{j}^{m})^{H} \mathbf{y}) - |\mathbf{y}_{1}|^{2} \right| \leq \delta, \tag{152}$$

for any $\mathbf{y} \in \mathbb{C}^N$ obeying $\|\mathbf{y}\| = 1$. Letting $\mathbf{y} = [\mathbf{y}_1, \tilde{\mathbf{y}}]$ where $\tilde{\mathbf{y}} \in \mathbb{C}^{N-1}$, and similarly partitioning the sampling vectors as $\mathbf{L}_i^m = [(\mathbf{L}_i^m)_1, \tilde{\mathbf{L}}_i^m]$ we have

$$\mathbf{y}^{H}\mathbf{L}_{i}^{m}(\mathbf{L}_{j}^{m})^{H}\mathbf{y} = (\mathbf{L}_{i}^{m})_{1}\overline{\mathbf{y}_{1}}(\overline{\mathbf{L}_{j}^{m}})_{1}\mathbf{y}_{1} + (\mathbf{L}_{i}^{m})_{1}\overline{\mathbf{y}_{1}}(\tilde{\mathbf{L}}_{j}^{m})^{H}\tilde{\mathbf{y}} + \tilde{\mathbf{y}}^{H}\tilde{\mathbf{L}}_{i}^{m}(\overline{\mathbf{L}_{j}^{m}})_{1}\mathbf{y}_{1} + \tilde{\mathbf{y}}^{H}\tilde{\mathbf{L}}_{i}^{m}(\tilde{\mathbf{L}}_{j}^{m})^{H}\tilde{\mathbf{y}}. \quad (153)$$

This yields

$$I_{0}(\mathbf{y}) = \left| \frac{1}{M} \sum_{m=1}^{M} (|(\mathbf{L}_{i}^{m})_{1}|^{2} |(\mathbf{L}_{j}^{m})_{1}|^{2} - 1) |\mathbf{y}_{1}|^{2} + |(\mathbf{L}_{i}^{m})_{1}|^{2} (\mathbf{L}_{j}^{m})_{1} \overline{\mathbf{y}_{1}} (\tilde{\mathbf{L}}_{j}^{m})^{H} \tilde{\mathbf{y}} \cdots \right.$$

$$\cdots + \left| (\mathbf{L}_{j}^{m})_{1} \right|^{2} (\overline{\mathbf{L}_{i}^{m}})_{1} \mathbf{y}_{1} \tilde{\mathbf{y}}^{H} \tilde{\mathbf{L}}_{i}^{m} + \overline{(\mathbf{L}_{i}^{m})_{1}} (\mathbf{L}_{j}^{m})_{1} \tilde{\mathbf{y}}^{H} \tilde{\mathbf{L}}_{i}^{m} (\tilde{\mathbf{L}}_{j}^{m})^{H} \tilde{\mathbf{y}} \right|$$

$$\leq \left| \frac{1}{M} \sum_{m=1}^{M} (|(\mathbf{L}_{i}^{m})_{1}|^{2} |(\mathbf{L}_{j}^{m})_{1}|^{2} - 1) |\mathbf{y}_{1}|^{2} \right| + \left| \frac{1}{M} \sum_{m=1}^{M} |(\mathbf{L}_{i}^{m})_{1}|^{2} (\mathbf{L}_{j}^{m})_{1} \overline{\mathbf{y}_{1}} (\tilde{\mathbf{L}}_{j}^{m})^{H} \tilde{\mathbf{y}} \right|$$

$$+ \left| \frac{1}{M} \sum_{m=1}^{M} |(\mathbf{L}_{j}^{m})_{1}|^{2} \overline{(\mathbf{L}_{i}^{m})_{1}} \mathbf{y}_{1} \tilde{\mathbf{y}}^{H} \tilde{\mathbf{L}}_{i}^{m} \right| + \left| \frac{1}{M} \sum_{m=1}^{M} \overline{(\mathbf{L}_{i}^{m})_{1}} (\mathbf{L}_{j}^{m})_{1} \tilde{\mathbf{y}}^{H} \tilde{\mathbf{L}}_{i}^{m} (\tilde{\mathbf{L}}_{j}^{m})^{H} \tilde{\mathbf{y}} \right|. \quad (154)$$

Due to the independence \mathbf{L}_i^m and \mathbf{L}_j^m , and from the fact that they are zero mean, unit variance i.i.d. Gaussian entry vectors, all four terms on the right-hand-side are measures of distance to expected values.

⁶Corresponds to Lemma 7.4 in the source material.

For the second and third terms, we have

$$\left| \frac{1}{M} \sum_{m=1}^{M} |(\mathbf{L}_{i}^{m})_{1}|^{2} (\mathbf{L}_{j}^{m})_{1} \overline{\mathbf{y}_{1}} (\tilde{\mathbf{L}}_{j}^{m})^{H} \tilde{\mathbf{y}} \right| \leq \frac{1}{M} \sqrt{\sum_{m=1}^{M} \left| |(\mathbf{L}_{i}^{m})_{1}|^{2} (\mathbf{L}_{j}^{m})_{1} \overline{\mathbf{y}_{1}} \right|^{2}} \sqrt{\sum_{m=1}^{M} \left| (\tilde{\mathbf{L}}_{j}^{m})^{H} \tilde{\mathbf{y}} \right|^{2}}$$

$$\leq |\mathbf{y}_{1}| \frac{1}{M} \sqrt{N \sum_{m=1}^{M} |(\mathbf{L}_{i}^{m})_{1}|^{4} |(\mathbf{L}_{j}^{m})_{1}|^{2}} \left(\frac{1}{\sqrt{N}} \sum_{m=1}^{M} \left| (\tilde{\mathbf{L}}_{j}^{m})^{H} \tilde{\mathbf{y}} \right| \right)$$

$$(155)$$

where the inequalities follow from Cauchy-Schwartz and $\ell_2 \leq \ell_1$. We then invoke Hoeffding's inequality from Proposition 10 in [68]. For any δ_0 and γ , there exists a constant $C(\delta_0, \gamma)$ such that $M \geq C(\delta_0, \gamma) \sqrt{N \sum_{m=1}^M |(\mathbf{L}_i^m)_1|^4 |(\mathbf{L}_i^m)_1|^2}$ where

$$\left| \frac{1}{M} \sum_{m=1}^{M} |(\mathbf{L}_{i}^{m})_{1}|^{2} (\mathbf{L}_{j}^{m})_{1} \overline{\mathbf{y}_{1}} (\tilde{\mathbf{L}}_{j}^{m})^{H} \tilde{\mathbf{y}} \right| \leq \delta_{0} \|\tilde{\mathbf{y}}\| |\mathbf{y}_{1}| \leq \delta_{0}, \tag{156}$$

with probability $1 - 3e^{-2\gamma N}$. For the final term, we invoke the Bernstein-type inequality of Proposition 16 in [68] per [1], such that for any positive constants δ_0 , γ , there exists the constant $C(\delta_0, \gamma)$ with

$$M \ge C(\delta_0, \gamma) \left(\sqrt{N \sum_{m=1}^{M} |(\mathbf{L}_i^m)_1|^2 |(\mathbf{L}_j^m)_1|^2} + N \max_{m=1\cdots M} |(\mathbf{L}_i^m)_1| |(\mathbf{L}_j^m)_1| \right)$$
(157)

where

$$\left| \frac{1}{M} \sum_{m=1}^{M} \overline{(\mathbf{L}_{i}^{m})_{1}} (\mathbf{L}_{j}^{m})_{1} \tilde{\mathbf{y}}^{H} \tilde{\mathbf{L}}_{i}^{m} (\tilde{\mathbf{L}}_{j}^{m})^{H} \tilde{\mathbf{y}} \right| \leq \delta_{0} \|\tilde{\mathbf{y}}\|^{2} \leq \delta_{0}$$

$$(158)$$

with probability $1 - 2e^{-2\gamma N}$.

To control the remaining terms, we use Chebyshev's inequality, per [1]. For any $\epsilon_0 > 0$ there exists a constant C with $M \geq C \cdot N$ such that the following hold

$$\left| \frac{1}{M} \sum_{m=1}^{M} (|(\mathbf{L}_{i}^{m})_{1}|^{2} |(\mathbf{L}_{j}^{m})_{1}|^{2} - 1) |\mathbf{y}_{1}|^{2} \right| \le \epsilon_{0} |\mathbf{y}_{1}|^{2}, \tag{159}$$

$$\left| \frac{1}{M} \sum_{m=1}^{M} (|(\mathbf{L}_{i}^{m})_{1}|^{4} |(\mathbf{L}_{j}^{m})_{1}|^{2} - 1) \right| \le \epsilon_{0}, \left| \frac{1}{M} \sum_{m=1}^{M} (|(\mathbf{L}_{i}^{m})_{1}|^{2} |(\mathbf{L}_{j}^{m})_{1}|^{4} - 1) \right| \le \epsilon_{0}$$
(160)

with probability at least $1-3N^{-2}$. Moreover, from union bound we have

$$\max_{m=1\cdots M} |(\mathbf{L}_{i,j}^m)_1| \le \sqrt{10\log M} \tag{161}$$

with probability at least $1-2N^{-2}$. As in [1], we denote the event that the results from Chebyshev's inequality hold by E_0 . Then, on event E_0 , combining all the terms, the inequality

$$I_0(\mathbf{y}) \le \epsilon_0 |\mathbf{y}_1|^2 + \delta_0 |y_1| \|\tilde{\mathbf{y}}\| + \delta_0 \|\tilde{\mathbf{y}}\|^2 \le \epsilon_0 + 2\delta_0, \tag{162}$$

holds with probability at least $1 - 8e^{-2\gamma N}$. We then follow by the ϵ -net argument of [1] via Lemma

5.4 in [68] to bound the operator norm such that

$$\max_{\mathbf{y} \in \mathcal{S}_{\mathbb{C}^N}} I_0(\mathbf{y}) \le \max_{\mathbf{y} \in \mathcal{N}} I_0(\mathbf{y}) \le 2\epsilon_0 + 4\delta_0, \tag{163}$$

where $\mathcal{S}_{\mathbb{C}^N}$ is the unit sphere in \mathbb{C}^N and \mathcal{N} is an 1/4-net of $\mathcal{S}_{\mathbb{C}^N}$. Then, choosing appropriate ϵ_0 , δ_0 and γ , and applying the union bound we have

$$\|\frac{1}{M}\sum_{m=1}^{M} \overline{(\mathbf{L}_{i}^{m})_{1}} (\mathbf{L}_{j}^{m})_{1} \mathbf{L}_{i}^{m} (\mathbf{L}_{j}^{m})^{H} - \mathbf{e}_{1} \mathbf{e}_{1}^{T} \| \leq \delta$$

$$(164)$$

with probability $1 - 8e^{-\gamma N}$ for $\delta = 2\epsilon_0 + 4\delta_0$, and

$$M \ge C' \left(\sqrt{N \sum_{m=1}^{M} |(\mathbf{L}_{i}^{m})_{1}|^{4} |(\mathbf{L}_{j}^{m})_{1}|^{2}} + \sqrt{N \sum_{m=1}^{M} |(\mathbf{L}_{i}^{m})_{1}|^{2} |(\mathbf{L}_{j}^{m})_{1}|^{2}} + N \max_{m=1 \cdots M} |(\mathbf{L}_{i}^{m})_{1}| |(\mathbf{L}_{j}^{m})_{1}| \right). \tag{165}$$

From E_0 , we have $M \ge C \cdot N$ which gives $M = \mathcal{O}(N \log N)$, where overall event holds with probability at least $1 - 8e^{-\gamma N} - 5N^{-2}$, hence, the proof is complete.